The impacts of warming on rapidly retreating high-altitude, low-latitude glaciers and ice core-derived climate records

Lonnie G. Thompson[a,b], Mary E. Davis[a], Ellen Mosley-Thompson[a,c],

Stacy E. Porter[a], Gustavo Valdivia Corrales[d,e], Christopher A. Shuman[f,g], Compton J. Tucker[f]

[a] Byrd Polar and Climate Research Center, The Ohio State University, Columbus OH 43210 USA

[b] School of Earth Sciences, The Ohio State University, Columbus OH 43210 USA

[c] Department of Geography, The Ohio State University, Columbus OH 43210 USA

[d] Consortium for the Sustainable Development of the Andean Ecoregion (CONDESAN), Calle Las Codornices 253, Lima 15047 Peru

[e] Facultad de Ciencias Sociales, Universidad Nacional Mayor de San Marcos, Ciudad Universitaria. Av. Venezuela Cdra. 34, Lima 15081 Peru

[f] Cryospheric Sciences Laboratory, NASA Goddard Space Flight Center, Greenbelt MD 20771 USA

[g] The Joint Center for Earth Systems Technology, University of Maryland, Baltimore County, Baltimore MD 21228 USA

Corresponding author: Lonnie G. Thompson (thompson.3@osu.edu)

Abstract

Alpine glaciers in the low and mid-latitudes respond more quickly than large polar ice sheets to changes in temperature, precipitation, cloudiness, humidity, and radiation. Many high-altitude glaciers are monitored by ground observations, aerial photography, and satellite-borne sensors. Regardless of latitude and elevation, nearly all nonpolar glaciers and ice caps are undergoing mass loss, which compromises the records of past climate preserved within them. Almost without exception, the retreat of these ice fields is persistent, and a very important driver is the recent warming of the tropical troposphere and oceans. Here we present data on the decrease in the surface area of four glaciers from low- to mid-latitude mountainous regions: the Andes of Peru and northern Bolivia, equatorial east Africa, equatorial Papua, Indonesia, and the western Tibetan Plateau. Climate records based on oxygen isotopic ratios ($\delta^{18}O$) measured in ice cores drilled from several glaciers in these regions reveal that the records from elevations below ~6000 meters above sea level have been substantially modified by seasonal melting and the movement of meltwater through porous upper firn layers. Fortunately, $\delta^{18}O$ records recovered from higher altitude sites still contain well-preserved seasonal variations to the surface; however, the projected increase in rate of atmospheric warming implies that climate records from higher elevation glaciers will eventually also be degraded. A long-term ice core collection program on the Quelccaya ice cap in Peru, Earth's largest tropical ice cap, illustrates that the deterioration of its climate record is concomitant with the increase in mid-troposphere temperatures. The melting ice and resulting growth of proglacial lakes presents an imminent hazard to nearby communities. The accelerating melting of glaciers, if sustained, ensures the eventual loss of unique and irreplaceable climate histories, as well as profound economic, agricultural, and cultural impacts on local communities.

Keywords

low-latitude glaciers, glacier retreat, ice cores, oxygen isotopes, climate change

1. Introduction

A vast amount of information about changing climatic and environmental conditions in low latitudes has been obtained from high-altitude glaciers (e.g., Mölg et al., 2003; Thompson et al., 2006, 2009, 2011a, 2018a, b; Racoviteanu et al., 2008; Bolch et al., 2012; Schauwecker et al., 2014, 2017; Tian et al., 2014; Seehaus et al., 2019). Glaciers serve as both recorders and sensitive indicators of climate change and are considered one of nature's best "thermometers" (Pollack, 2010), as they integrate and respond to most key climatological variables such as temperature, precipitation, cloudiness, humidity, and radiation. Due to their relatively small size compared to polar ice sheets, the tropospheric warming since the mid-20th

century has had devastating effects on alpine glaciers and ice caps. Various 21st century studies have concluded that many may disappear during this century if the current rates of retreat continue or accelerate (Thompson et al., 2006, 2011a, b; Rabatel et al., 2013; Albert et al., 2014; Permana et al., 2019). In the Americas and South Asia, the regions containing most of Earth's low-latitude ice, total glacier volume in 56 glacierized drainage basins is predicted to decrease by 43±14% (Representative Concentration Pathway, or RCP 2.6) to 74±11% (RCP 8.5) (Huss and Hock, 2018). This alpine glacier retreat is exacerbated by elevation dependent warming (EDW), the rate of which varies at different altitudes (Bradley et al., 2006; Qin et al., 2009; Pepin et al., 2015, 2019; Aguilar-Lome et al., 2019).

The effects of the recent warming on many low-latitude (30°N to 30°S) glaciers are further enhanced by their location in monsoon regions, which are impacted either directly or indirectly by the linked atmosphere/ocean phenomenon known as El Niño-Southern Oscillation (ENSO) (e.g., Paegle and Mo, 2002; Shaman and Tziperman, 2004; Gadgil et al., 2007; Abram et al., 2009). During warm ENSO events ("El Niño") heat spreads uniformly throughout the Tropics (Chiang and Sobel, 2002), and particularly strong warm or cold events ("La Niña") can immediately affect the surface area and thickness of many low-latitude alpine glaciers (Thompson et al., 2017; Permana et al., 2019; Veettil and Simões, 2019). As mountain glaciers are highly sensitive to changes in temperature and precipitation, their responses to the recent global-scale warming are early indicators of the fate of mountain and downstream-related hydrology, ecosystems, and biodiversity in regions where 40% of Earth's population resides (Beniston, 2003; Huss et al., 2017; Huss and Hock, 2018; Milner et al., 2017; Cauvy-Fraunié and Dangles, 2019; Yao et al., 2019; Stibal et al., 2020).

Using satellite imagery to determine surface area changes of selected alpine glaciers and records of stable isotopes of oxygen in ice cores, we discuss the changes observed on many low- and mid-latitude (between 35°N and 18°S) alpine glaciers over the last several decades. For example, observations from Quelccaya, the Earth's largest tropical ice cap located in the Andes of southern Peru, demonstrate how the recent warming at higher elevations has resulted in ice melt from both the surface and the margins. This melt has affected both the ice core climate records and environmental conditions near the ice cap which have impacted local communities.

The glaciers discussed here have been monitored and/or drilled over recent decades so that changes in their size and in the physical and chemical properties of the snow and ice are well documented (Thompson et al., 2011a, 2017; Cullen et al., 2013; Permana et al., 2019). The ice core records have previously been published individually as time averages (annual to multi-centennial); however, here the focus is to compare changes in the intra- and inter-seasonal variations in the most recent portions of the records with those in the deeper and older sections.

2. Materials and Methods

2.1. Stable isotopes of oxygen ($\delta^{18}O$)

Since 1974 the Byrd Polar and Climate Research Center at The Ohio State University (BPCRC-OSU) has undertaken a program of sample collection from pits, shallow cores, and deep cores from high-altitude, low-latitude glaciers and ice fields. These include glaciers and ice caps in the Andes of Peru and northern Bolivia, the Tibetan Plateau and the Himalayas, the summit of Kibo on Mt. Kilimanjaro in Tanzania, and the ice fields near Puncak Jaya in Papua, Indonesia. Although all ice core and pit samples were analyzed for multiple chemical parameters, the measurement that all have in common is $\delta^{18}O$ (stable isotopic ratios of ^{18}O to ^{16}O). The $\delta^{18}O$ of snow, firn, and ice samples were measured at BPCRC-OSU using Thermo Finnigan mass spectrometers, which were later replaced by PICARRO cavity ring-down spectroscopy analyzers.

2.2 Ice core dating

Most ice cores from high precipitation regions with distinct wet and dry seasons contain well-defined oscillations in $\delta^{18}O$ and the concentrations of dust and major anions and cations that are derived from soluble aerosols. Where these seasonal variations are discernible, they can be counted and dated. As snow accumulates it is compressed and metamorphosed into firn and then into ice containing annual layers that thin with depth and are often identifiable by seasonal oscillations in aerosols and stable isotopes (e.g., Thompson et al., 2000, 2013). The $\delta^{18}O$ profiles presented here from the Andes and the western Tibetan Plateau (except for Naimona'nyi in the western Himalayas) have been dated back to 1800 CE by counting these wet/dry season oscillations. The dating of the Naimona'nyi core is discussed in section S1 of the Supplement. The much more challenging time scale construction of the climate records from the inner tropical (3°S to 4°S) glaciers on Kilimanjaro, Tanzania and in Papua, Indonesia, required additional techniques that are described in Thompson et al. (2002) and Permana et al. (2019), respectively.

2.3 Glacier and ice field surface area measurements

Surface areas of glaciers on Kilimanjaro (Tanzania), Naimona'nyi (western Himalayas, Tibetan Plateau), Quelccaya (southern Peru), and near Puncak Jaya, Papua, Indonesia (Fig. 1A-D), were determined using the Landsat Glacier Retrospective analysis. This method targets specific, distinct ice areas, ice caps, and entire cordilleras that are intermittently snow- and cloud-free throughout the nearly 50-year span of Landsat imagery. By selecting appropriate imagery when available over the nearly five decades of archived and publicly accessible Landsat imagery, the limited and lower temporal and spatial resolution Multi Spectral Scanner images can readily be contrasted with the more recent and higher spatial and spectral resolution Thematic Mapper, Enhanced Thematic Mapper Plus, and Operational Land Imager imagery. Because the key short-wave infrared, near infrared, and Green bands have been carried on every Landsat sensor, it is possible to clearly visualize glacial ice area changes over the last ~50 years. By utilizing an unsupervised classification algorithm within a global information system program on these geo-referenced images, it is possible to generate ice area estimates over time. Descriptions of imagery selection, analysis, and uncertainty estimation are provided in the Section S2 of the Supplement.

3. Climatic interpretation of $\delta^{18}O$

The isotopic composition of oxygen in precipitation is calculated as the difference between the isotopic ratio of the precipitation (R_{spl}) and a standard (R_{std}), usually standard mean ocean water (SMOW), in the equation:

$$\delta^{18}O = \left(\frac{R_{spl} - R_{std}}{R_{std}}\right) x\ 10^3,$$

which is expressed as per thousand or per mille (‰). Oxygen isotope values of tropical ocean surface water vary between 0‰ and 2‰ (Schmidt et al., 1999), and vapor directly from the ocean source is more enriched in the lighter isotope (^{16}O), which evaporates more readily than the heavier isotope (^{18}O). As the vapor is transported and condenses to form precipitation, ^{18}O is more readily removed from the vapor, the reverse of the evaporation process. If the moisture continues to travel over land where less evaporation occurs, the water vapor becomes further depleted in ^{18}O and the $\delta^{18}O$ values in the precipitation become more negative.

This is a very simple explanation of oxygen isotopes in precipitation. However, the interpretation of atmospheric influences on $\delta^{18}O$ in precipitation is both complex and controversial. In the extratropical regions there is a direct relationship between $\delta^{18}O$ and temperature (Schmidt et al., 2007), but in the Tropics the relationship is more strongly correlated with the "amount effect" (Rozanski et al., 1993; Schmidt et al., 2007), especially in monsoon regions with strong seasonal precipitation variations. The amount effect implies that $\delta^{18}O$ values in precipitation become more negative (less ^{18}O enriched) as large amounts of moisture condense in (and fall from) clouds, thereby initially removing the heavier ^{18}O. As condensation continues the remaining water vapor and precipitation become progressively more depleted in ^{18}O. Thus, in monsoon regions $\delta^{18}O$ values tend to be lower during the summer monsoon season than during the dry winter. In reality, controls on $\delta^{18}O$ are much more complicated, and include atmospheric temperature and pressure at different altitudes, sea surface temperatures, precipitation pathways (i.e., over land or over water), the ratio of stratiform vs. convective precipitation, and the amount of moisture recycling during transport (Pang et al., 2011; Hurley et al., 2015; Aggarwal et al., 2016; Cai and Tian, 2016; Thompson et al., 2017). The link between oceanic and middle to upper atmosphere temperatures and wet season $\delta^{18}O$ in the tropical monsoon regions may be through convection, in which condensation occurs much higher in the atmosphere where temperatures are lower. More intense convection, which is driven by higher temperatures at and near the surface, occurs higher in the atmosphere (Permana et al., 2016; Thompson et al., 2017).

4. Recent changes in retreating alpine glaciers: mass loss and ice core-derived climate records

Nearly all of Earth's high-altitude, low- and mid-latitude glaciers are losing mass, and since the beginning of the 21st century the rates of ice loss have been at historically unprecedented levels (Zemp et al., 2015). These include glaciers and ice caps that researchers from BPCRC-OSU have drilled and monitored over several decades. The ice retreat histories during the late 20th and early 21st centuries for four of the sites discussed in this study are shown in Fig. 1 and Table S1, Supplement. According to the data from the Landsat Glacier Retrospective analysis (Table S1), the ice surface area loss by percent is greatest at the inner tropical sites of Papua at 4^{o}S (~93% loss in 39 years) and Kilimanjaro at 3^{o}S (~71% loss in 32 years) and least (by percent) on Naimona'nyi at 30^{o}N (~9% loss in 39 years). Stable isotope data from pits and cores collected at these sites, many at the same location over multiple years, illustrate the changes in the upper layers of these glaciers. These results are presented below by region.

4.1. Glaciers in the Peruvian and northern Bolivian Andes

The precipitation in the Andes of Peru and Bolivia is dominated by the "South American Monsoon System" (SAMS), which matures from December to February. Briefly, the SAMS is characterized by deep convection over the Amazon Basin, the latent heat from which is instrumental in the development of the Bolivian High in the upper troposphere (Lenters and Cook, 1997). North of the high, northeasterlies carry moisture originating in the tropical North Atlantic over the Amazon Basin to the tropical and subtropical Andes (Garreaud et al., 2003). After the monsoon season the core of convection moves northward, and the tropical moisture to the Andes is shut off. The "outer tropical" Andes, which include Peru and Bolivia, experience distinct seasonality in precipitation, receiving most of the annual precipitation during the wet season between October and April (Veettil et al., 2017). The inner Tropics, which lie within the migration boundaries of the Intertropical Convergence Zone (ITCZ), experience only minor seasonal variations in precipitation. Temperatures over glaciers in the outer Tropics range from less than 5°C between winter and summer in the Cordillera Blanca (~9°S to 10°S) (Schauwecker et al., 2014) to 8°C on Nevado Sajama at 18°S on the Altiplano in northern Bolivia (Hardy et al., 2003).

Since 1974 BPCRC-OSU has drilled and monitored several ice caps and glaciers in the outer tropical Andes (Fig. 2) from 9°S to 18°S and at altitudes between 5060 and 6540 meters above sea level (masl). These include sites in the Cordillera Blanca in northern Peru (Fig. 2, map inset), the Quelccaya and Coropuna ice caps in southern Peru, and the Sajama ice cap on the Bolivian Altiplano. Here we review recent mass loss in the outer tropical Andes and present seasonally-resolved climate records from these glaciers dating from the late 20th to the early 21st century.

4.1.1 Mass loss of outer tropical Andean glaciers

Analyses of ice mass loss along the entire Andes Mountains (10°N to 56°S) from 2000 to 2018 show that glaciers in the combined inner and outer Tropics lost 0.42 ± 0.24 m water equivalent (w.e.) a^{-1}, exceeded only by the loss rate in the Patagonian region (0.78 ± 0.25 m w.e. a^{-1}) (Dussaillant et al., 2019). Among the outer tropical sites from which ice cores have been recovered by BPCRC-OSU, the ice cover on Nevado Coropuna (15.54°S) decreased from 58.0 to 44.1 km^2 (or by ~0.71% a^{-1}) between 1980 and 2014 (Kochtitzky et al., 2018), while the snowline altitude on two Sajama outlet glaciers (18.11°S) increased by ~400 m and ~640 m between 1984 and 2011 (Veettil et al., 2016). On Nevado Huascarán (9.11°S), the Earth's highest tropical mountain, debris-free glaciers decreased in area by 18.67% from 1970 to 2003, consistent with the retreat rate during the previous half-century (Racoviteanu et al., 2008). Although the Huascarán ice is currently retreating more slowly than lower elevation glaciers, as the freezing level height (FLH) rises this mountain will also undergo dramatic ice melt and loss. In addition, exposure of the darker surface as the ice retreats will decrease the albedo and enhance surface heat absorption and radiative flux (Pepin et al., 2015), as illustrated in a photograph of Huascarán taken during the dry season of 2019 showing the exposure of fresh rock as the ice retreats (Fig. 3).

The surface area of Quelccaya decreased by 46% between 1976 and 2020 (Fig. 1C), and this has been attributed to increasing air temperature rather than decreasing precipitation, as the latter did not significantly change over this period (Yarleque et al., 2018). Glacier retreat rates in Peru are greatly accelerated during strong El Niño events (Seehaus et al., 2019). However, glacier surface areas are also affected immediately by both El Niño and La Niña events, as shown by measurements on a glacier on Nevado Champara in the Cordillera Blanca, where a small recovery was measured during the 2016/17 La Niña after the retreat in snow/ice cover due to the warming of the 2015/16 event (Veettil and Simõas, 2019). Nevertheless, such short-term recoveries are not sufficient to reverse the effects of the increasing air temperature trend in the outer tropical Andes. Yarleque et al. (2018) calculated that air temperature above Quelccaya could increase 2.4ºC (RCP 4.5) to 5.4ºC (RCP 8.5) by the end of the century, and under the latter scenario Quelccaya, Earth's largest tropical ice cap, will continue to lose mass until it eventually disappears.

4.1.2 Records of recent climate change from the outer tropical Andes

The $\delta^{18}O$ profiles from the deep cores (drilled to bedrock) recovered by BPCRC-OSU in the outer tropical Andes, arranged from north to south (black broken line in Fig. 2), are shown in Fig. 4 for two time slices, from 1800 to 1850 CE and from 1950 CE to the top of each record. The higher (>6000 masl) and lower elevation (<6000 masl) ice core records demonstrate differences in both the $\delta^{18}O$ inter-seasonal variations and the mean values (Table 1) between the early 19th (1800 to 1850 CE) and post 1950 CE time slices. Note that all five profiles show recent $\delta^{18}O$ increases. Except for Coropuna, which is discussed below, the greatest increases occur in the data from the lower elevation sites of Hualcán (+0.99‰) and Quelccaya (+1.23‰), where the recent isotopic smoothing is most obvious (Fig. 4). The profiles from two of the higher elevation sites (Huascarán and Sajama) maintain distinctive wet and dry season variations to the surface at the time they were drilled, and the mean values are consistent between the two periods (+0.11‰ and +0.20‰, respectively).

An exception to the relationship of ^{18}O depletion with altitude toward the present is evident in the record from the ice core drilled at the summit of Coropuna (6450 masl), which shows a 1.27‰ increase despite the persistence of $\delta^{18}O$ seasonal oscillations towards the present. However, a shallow core drilled at a lower elevation (6080 masl) site on Coropuna in the same year shows smoothing of the $\delta^{18}O$ signal below ~6 m depth (Herreros et al., 2009). Average $\delta^{18}O$ values from the summit may show a larger difference between these two time slices because, like Quelccaya, it contains a more distinctive expression of the "Little Ice Age," a multi-centennial cooling that occurred from ~1300 to ~1850 CE. Paleoclimate and historical records from around the world show different timings and durations of the cooling, and there is little consensus among climatologists regarding its primary cause (Matthews and Briffa, 2005). Although the Little Ice Age is regarded as primarily a Northern Hemisphere phenomenon, it has been identified in some Southern Hemisphere paleorecords such as those from Quelccaya (Thompson et al., 1986; 2013).

	Coordinates	Elevation masl	1800-1850 CE $\delta^{18}O$ (‰)	Post-1950 CE $\delta^{18}O$ (‰)	Difference (‰)	Year of core drilling
Andes						
Huascarán	9.11°S; 77.61°W	6050	-17.56	-17.45	+0.11	2019
Hualcán	9.26°S; 77.50°W	5400	-16.42	-15.43	+0.99	2009
Quelccaya	13.93°S; 70.83°W	5670	-18.60	-17.37	+1.23	2003
Coropuna	15.54°S; 72.65°W	6450	-19.22	-17.95	+1.27	2003
Sajama	18.11°S; 68.88°W	6540	-17.32	-17.12	+0.20	1997

Table 1. Average $\delta^{18}O$ values during 1800-1850 CE and post 1950 CE time slices, and the differences between them, in low-latitude ice cores from the outer tropical Andes.

A detailed view of $\delta^{18}O$ data from five glaciers in the Cordillera Blanca (Fig. 2, inset) demonstrates how the recent warming has affected the preservation of the climate records in the upper layers of these ice fields over the past four decades (Fig. 5). The $\delta^{18}O$ data shown for these eight cores drilled between 1984 and 2019 are from samples above the firn/ice transition. Similar to the records in Fig. 4, these profiles are arranged from north to south in line with a cross section along the axis of the mountain range (yellow broken line in Fig, 2, inset). The shallow core drilled on Pucahirca in 1984 exhibits a pronounced wet season ^{18}O depletion (more negative δ^{18}O) in the fresh snow in the top 3 meters; however, the amplitude decreases below the 1983/84 annual layer indicating that surface melting was already underway. Six years later the δ^{18}O seasonality, even in the most recent year's snow accumulation, was completely "washed out." The Hualcán, Copap, and Caullaraju cores drilled in 1990-91 show no seasonal variations; however, the Hualcán core drilled 130 meters higher in 2009 still shows some seasonality only in the top 10 meters. The only glacier that maintains an intact climate record is on the col of Huascarán. From 1993, when the col ice was first drilled, to the most recent record from a core drilled in 2019, the distinctive seasonal oscillations persist because the lower temperatures at its higher altitude prevent significant melting.

Just as for other high precipitation tropical regions, the interpretation of stable isotopes in outer tropical Andes glaciers is controversial, particularly concerning whether temperature or precipitation amount is determinative. Stable isotope values in Andean ice cores from the outer Tropics have a positive correlation with tropical middle troposphere temperatures (Thompson et al., 2017). However, other studies indicate that the amount effect is of primary importance during the monsoon season (Vuille et al., 2003; Hurley et al., 2015). Other potential influences involve upstream processes such as convection over the Amazon Basin during the austral wet summer (Risi et al., 2008; Samuels-Crow et al., 2014), tropical North Atlantic sea surface temperatures, and upper atmospheric conditions in the equatorial Pacific (Thompson et al., 2017). However, regardless of the processes involved in the production of the seasonal values of stable isotopes in the Andean ice cores, the obliteration of the oscillations in these lower altitude ice cores is almost certainly the result of rising temperatures and the resulting snow melt at the glacier surface and the movement of meltwater downward through the firn. Although seasonal temperature differences are much smaller than seasonal precipitation, the increasing intensity in surface melt may be caused by a combination of rising FLH which is related to the warmer tropical tropospheric and sea surface temperatures (Thompson et al., 2017), and by changes in austral summer cloud cover (Imfeld et al., 2020).

If atmospheric temperatures and the FLH continue to rise, the climate records from Huascarán will likely encounter the same fate as the records from its lower elevation neighbors. Between the most optimistic and the most pessimistic CMIP5 RCP scenarios, FLH in the Peruvian Andes, including the Cordillera Blanca, will increase by 230 to 850 m by the end of the 21st century (Schauwecker et al., 2017). However, since air temperature and FLH are also influenced by El Niño, projected changes in its frequency and intensity may also alter these rates, although forecasts of ENSO behavior and its relationship with anthropogenic forcing are inconsistent (Maher et al., 2018; L'Heureux et al., 2020).

4.1.3 Ice core evidence linking melting on Quelccaya with atmospheric warming

Few low-latitude alpine glaciers have received more attention or have been sampled more frequently than the Quelccaya ice cap. Changes at the summit over the last four decades have been documented by a series of shallow cores drilled and analyzed for $\delta^{18}O$ (Fig. 6A). Melting on the summit was minimal in 1976; however, just three years later some evidence of melting and water movement through the firn was already apparent and progressed rapidly thereafter. Subsurface water was first noticed at the summit during drilling in the early 1980s (Thompson et al., 2017), and by 1991 the seasonal $\delta^{18}O$ variations were almost completely "washed out," consistent with observations in the Cordillera Blanca records (excluding Huascarán) from the early 1990s (Fig. 5). A time series of reanalysis mid-troposphere (500 mb) annual temperatures near Quelccaya from 1975/76 to 2017/18 shows a warming trend which is augmented by strong El Niño events in 1982/83, 1997/98, 2009/10, and 2015/16 (marked by red closed circles in Fig. 6B). Strong El Niño events are characterized by unusually high tropical Pacific SSTs and upper atmospheric warming, increasing FLH (Bradley et al., 2009), and mass balance decreases (Vuille et al., 2008). The temperature in 1978/79, when intense attenuation of the seasonal $\delta^{18}O$ was first noticed, is marked by a broken line in Fig. 6B and illustrates that mid-troposphere temperature over Quelccaya has remained above that level since 1999/2000. Not only did the temperature over Quelccaya reach that threshold in 1999/2000, but the rate of temperature increase almost quadrupled during the following two decades (0.044^{o}C a^{-1}) compared with the previous quarter century (0.012^{o}C a^{-1}). As the local 500 mb temperature continued to increase after 2003, the $\delta^{18}O$ profiles show decreasing seasonality, even within the snowfall of the most recent year (~3 meters) in each record. Melting on the ice cap became more pronounced and in 2016 members of a BPCRC-OSU expedition observed water on the surface near the summit in response to warming from the 2015/16 El Niño (Thompson et al., 2017). The tropical warming of the 2015/16 El Niño is manifested in the Quelccaya summit snow as the complete absence of $\delta^{18}O$ seasonality; however, a shallow core drilled in July 2018 shows some recovery resulting from La Niña cooling.

4.1.4 Impacts of the melting of Quelccaya and resulting GLOFs on local communities

Events in recent decades around the Quelccaya ice cap exemplify the impact of glacier melt on nearby communities and confirm the value of the long-term program of ice core collection on Quelccaya that demonstrates the progression of the ice melt that preceded the events described below. In March 2006, an ice avalanche fell into the lake formed by the meltwater from the retreating Qori Kalis outlet glacier (Fig. 7) and created a small tsunami that produced a sudden flooding of the area below the lake and drowned grazing livestock along the outlet stream (Thompson et al., 2011a). In December 2007, another proglacial lake located 3.5 km to the south of Qori Kalis generated a glacial outburst flood (GLOF) which traveled ~6 km southwestward within a valley and overwhelmed the small community of Phaco (Fig. 7). Fortunately, there were no human fatalities, although it affected a large area, destroyed fences and pastures, and killed several animals. When local residents backtracked the source of the flood, they observed large pieces of ice in the proglacial lake and concluded that, like the 2006 GLOF, the outburst was caused by calving of ice from the retreating margin of Quelccaya into that lake. A resident of nearby Phinaya who was interviewed by co-author G.V.C. described this event as completely unexpected and impacting a community that was unprepared to deal with its consequences (Supplement, Section S3). The climatic precursors that were instrumental in the occurrence of these floods had been forming for several years. From the late 1990s to the mid-2000s the total area of proglacial lakes along the western margin of Quelccaya increased rapidly (Hanshaw and Bookhagen, 2014) as the rate of mid-troposphere temperature warming increased (Fig. 6B). While these proglacial lakes were growing during the four years before the March 2006 Qori Kalis GLOF and for six years before the December 2007 Phaco GLOF, the $\delta^{18}O$ profiles from shallow cores drilled from 2004 to 2007 show nearly complete obliteration of the climate signal at the summit of Quelccaya (Fig. 6B). These data and observations lead to the conclusion that Quelccaya is melting not only at the margins but at the summit as the result of persistent warming, which accelerated the growth of lakes around the margins and exacerbated the threat to nearby populations.

What is happening on and around Quelccaya is an example of potential hazards throughout the tropical Andes as glaciers melt and proglacial lakes form and grow. These conditions are particularly hazardous in and below rugged, high relief terrain such as the Cordillera Blanca, where ice cores drilled on several glaciers show persistent melting over recent decades (Fig. 5). Populations in areas that are vulnerable to geohazards such as glacial lake outburst floods (GLOFs) have increased substantially in the last century. For example, changes in the extensively studied proglacial Lake Palcacocha below the Palcaraju glacier, the source of a GLOF that destroyed a large portion of the city of Huaraz in 1941, has a significant potential of flooding again as a result of the recent warming that is contributing to the retreat of the glacier and the growth of the lake (Stuart-Smith et al., 2021).

4.2 Glaciers in the inner Tropics

Whereas precipitation on outer tropical glaciers is seasonally variable, glaciers and ice fields in the inner Tropics are directly influenced by the latitudinal movement of tropical convection associated with the ITCZ and thus receive precipitation almost year-round, although normally there are two maxima. The mass balance of inner tropical glaciers is highly sensitive to changes in temperature and to ENSO (Veettil et al., 2017, Permana et al., 2019) and thus are at greater risk from persistent warming. Inner tropical ice fields at two locations have been drilled and monitored by BPCRC-OSU and colleagues. These are on Kilimanjaro in equatorial East Africa and near the Puncak Jaya peak in Papua, Indonesia, and they are retreating at faster rates than larger glaciers located at higher latitudes such as Quelccaya and Naimona'nyi in the Himalayas (Fig. 1).

4.2.1 Kilimanjaro, Tanzania, East Africa

In equatorial East Africa glaciers currently exist in only three locations: on Mt. Kenya (Kenya), on Mt. Kilimanjaro (Tanzania), and in the Ruwenzori range (Uganda). Of all these sites, glaciers in the Ruwenzori range have been least studied; however, from 1987 to 2003 the ice extent there halved from 2.01 ± 0.56 km^2 to 0.96 ± 0.34 km^2 (Taylor et al., 2006), and the glaciers have been projected to disappear within the first quarter of this century. Mt. Kenya lost 44% of its ice cover between 2004 and 2016, and after 2010 the loss of its largest glacier accelerated as it split apart (Prinz et al., 2018). Similar to the Ruwenzori glaciers, the ice on Mt. Kenya has been projected to disappear within ten years if this rate of retreat persists.

Of the glaciated mountains in East Africa, Kilimanjaro (3^{o}S) is arguably the most famous and most iconic. Although the ice fields on Kilimanjaro (Fig. 1A) do not directly affect water supplies for nearby communities (Mölg et al., 2013), they are nevertheless of vital importance to the economy of Tanzania, as tourism in the Kilimanjaro National Park contributes 13% to the country's gross domestic product (Christie et al., 2013). Tourism on Kilimanjaro is dependent on climate conditions. The mountain contains several climate zones, with varying precipitation and temperature, from rainforest in the lower slopes to arctic at the summit. The zone above 4000 masl receives only 20% of the precipitation received on the southern slope at 2400 masl (Hemp, 2006). Automated weather station data indicate that between 2005 and 2013 snowfall averaged 570 mm w.e. a^{-1} near the summit (Collier et al., 2018).

In 2000 several ice cores were drilled on the Kilimanjaro ice fields by BPCRC-OSU. Although shallow cores (11 and 13 m long) were recovered from the Lewis glacier on Mt. Kenya (Thompson, 1978), those from Kilimanjaro are the only existing ice cores recovered to bedrock from the equatorial East African glaciers. The oldest climate records from these cores extend back ~11.7 ky BP (Thompson et al., 2002);

however, these records end before 2000 CE as the ice fields have thinned from the surface downward (Thompson et al., 2002). An example of the condition of the ice core climate records is illustrated by the $\delta^{18}O$ profile from the Furtwängler glacier (FWG) (Fig. 8A). When it was drilled in 2000, the FWG was a thin (10 m), water-saturated ice mass in the middle of the Kibo crater. Although the bottom of the core is dated ~1680 CE (see Supplementary Information and Fig. 3 in Thompson et al., 2002), at the time of drilling the melting and sublimation had removed the top layers of ice and smoothed high-resolution $\delta^{18}O$ variations. The upper 2.5 meters show steady ^{18}O enrichment, possibly in response to increasing temperature and/or aridity.

Similar to nearly all the tropical cryosphere, the multiple ice fields on the summit of Kilimanjaro (3°S) are also rapidly disappearing (Fig. 1A). Satellite images, aerial photographs, and field measurements taken over the last three decades on the Kibo crater show that the ice fields have diminished in surface area (Fig 1A) and thickness (Thompson et al., 2011b). Between 2000 and 2009 the thickness of the FWG decreased by ~50% (Thompson et al., 2009). In 2007 sublimation and melting caused the ice field to split into two parts, and between 2010 and 2017 its surface area halved (Lamantia, 2018). In 2000 a stake was placed in the ice core borehole where the FWG's ice thickness decreased by ~0.5 meter/year until 2013, when that portion of the ice field disappeared revealing the bottom of the stake and the bedrock beneath (D. R. Hardy, personal communication).

The much larger Northern ice field (NIF) had a maximum thickness of ~50 meters in 2000, but by 2007 it had thinned by 1.9 meters. Like the FWG, by 2012 it had bifurcated into two ice fields. Readings from energy-balance stations installed on the NIF show that daytime irradiance on the ice surface exceeds the limit required to drive ice melting (Thompson et al., 2011b).

4.2.2 Papua, New Guinea, Indonesia

Eleven thousand km east of Kilimanjaro, ice fields near Puncak Jaya (Carstensz Pyramid) (4°S) in Papua, New Guinea, Indonesia were drilled to bedrock in 2010 by BPCRC-OSU. At 4884 masl, Puncak Jaya is the highest peak between the Himalayas and the Andes. Papua is located in the West Pacific Warm Pool (WPWP), where sea surface temperatures constantly exceed 28ºC. Its precipitation and temperature are greatly affected by ENSO (Prentice and Hope, 2007). The climate of Papua is very wet, with rainfall amounts averaging ~2500 to 4500 mm a^{-1} (Prentice and Hope, 2007) and a maximum of 12,500 mm measured at 617 masl (Permana et al., 2016). Precipitation is almost seasonally constant at high altitudes, characterized by a wet season during the austral summer (December to March) and a “less wet” season during austral winter (May to October) as the ITCZ passes overhead twice a year (Prentice and Hope, 2007; Permana et al., 2016).

Like the Kilimanjaro ice cores, the cores recovered from the Papua ice fields are the only ones in existence. Due to the large annual precipitation rate and the thinness of the ice (~32 m maximum), the climate record is relatively short, possibly extending back only to the early 20th century (Permana et al., 2019). The $\delta^{18}O$ profile shows deterioration of the climate signal (Fig. 8B). As in the record from the FWG on Kilimanjaro, the upper meters are characterized by smoothed ^{18}O enrichment (less negative $\delta^{18}O$ values). A study of $\delta^{18}O$ on precipitation samples collected at various altitudes along the southern slope of the Papua mountain ranges concluded that $\delta^{18}O$ values are controlled by condensation temperatures associated with convection levels in the troposphere (Permana et al., 2016). The increasing $\delta^{18}O$ reflects ENSO-related atmospheric and sea surface warming trends in the WPWP region, which are directly responsible for the rapid shrinking and thinning of the ice fields (Fig. 1D). The effect of El Niño on the Papua ice fields was confirmed by satellite imagery analysis and accumulation stake measurements conducted since 2010, which showed that reduction in surface area and thickness intensified during the strong 2015/16 event (Permana et al., 2019). Disappearance of all the ice in this region is projected to occur within a decade, assuming the current rate of retreat persists.

4.3 Glaciers in the western Tibetan Plateau and Himalayas

The climate conditions on the Tibetan Plateau, are quite different from those in the Peruvian Andes or the inner Tropics. This region is influenced by several air masses (Fig. 9) which vary spatially and temporally. Along its southern border the Tibetan Plateau receives most of its snowfall from the Indian and Southeast summer monsoons, although the continental westerlies also contribute moisture in the winter. North of the Himalayas the climate is more arid, and glaciers receive less snowfall which is derived primarily from the westerlies and from recycled moisture originating from thunderstorms in the summer (Fu et al., 2006; Thompson et al., 2018b). Unlike the outer tropical Andes, there are large seasonal temperature differences (16-17°C in 2011 CE, Duan et al., 2017) on the Tibetan Plateau.

Stable isotopes of precipitation in the Tibetan Plateau cryosphere have been extensively studied, and there is a consensus that temperature is a major influence on δ^{18}O values in the arid north and west on seasonal and interannual timescales (Yao et al., 2013, Thompson et al., 2018b; Yu et al., 2020; Pang et al., 2020). Stable isotopes in the north are higher/lower in summer/winter precipitation, but in the monsoon domain of the central and eastern Himalayas, the seasonal variations in δ^{18}O resemble those of the tropical Andes, i.e., higher/lower values in the dry winter/wet summer (Thompson et al., 2000; Yao et al., 2013). On decadal and longer timescales, the δ^{18}O records may be more reflective of temperature throughout the region (Thompson et al., 2000; Yu et al., 2020). Controversy about this interpretation remains, as stable isotope model results indicate that δ^{18}O is controlled by monsoon intensity (Vuille et al., 2005) on all timescales.

The Guliya ice cap in the Kunlun Mountains is located in the arid northwestern region, while the Naimona'nyi and Dasuopu glaciers are located in the western and central Himalayas, respectively (Fig. 9). Profiles of δ^{18}O for two time slices, between 1800 and 1850 CE, and post 1950 CE, are shown in Fig. 10A. All three drill sites are located above 6000 masl. The increases between the 1800 to 1850 CE and the post 1950 CE (Table 2) periods are larger than those in the Andean δ^{18}O records, although the latter show greater variability in isotopic enrichment (Table 1). Precipitation varies widely by latitude, and Guliya at 35°N has a net ice accumulation rate of only ~200 mm a^{-1}, while Dasuopu at 28°N in the Himalayas has a net accumulation rate of ~1000 mm a^{-1}. However, the Naimona'nyi glacier in the Himalayas is losing rather than accumulating ice at the surface, and by 2006 it had lost almost 50 years of its climate history (Fig. 10A). This was first reported by Kehrwald et al. (2008), who noted that the Naimona'nyi ice cores lack the elevated 1962/63 CE beta emission levels that are artifacts of atmospheric bomb testing in the Soviet Arctic and occurs in all the ice cores drilled by BPCRC-OSU in the Himalayas and on the Tibetan Plateau (Kehrwald et al., 2008). This loss is illustrated more directly in Fig. 10B, which compares the climate record of annually averaged $\delta^{18}O$ among Guliya (Thompson et al., 2018b), Dasuopu (Thompson et al., 2000), and Naimona'nyi after 1900 CE. Although these glaciers are located several hundred kilometers apart and in regions with different precipitation regimes, their post 1900 CE $\delta^{18}O$ trends are similar at annual resolution. All three sites receive most of their precipitation in the summer; however, the $\delta^{18}O$ values in the Himalayan records are lower than those in the Guliya record due to their closer proximity to the monsoon moisture source. Much of the snow that falls on Guliya comes from water vapor that is recycled through Central Asia (Thompson et al., 2018b), resulting in higher $\delta^{18}O$ values.

	Coordinates	Elevation masl	1800-1850 CE $\delta^{18}O$ (‰)	Post-1950 CE $\delta^{18}O$ (‰)	Difference (‰)	Year of core drilling
Tibetan Plateau						
Guliya	35.13ºN; 81.38ºE	6200	-14.65	-12.20	+2.45	2015
Naimona'nyi	30.45ºN; 81.33ºE	6050	-18.37	-------	-------	2006
Dasuopu	28.38ºN; 85.72ºE	7200	-20.04	-17.96	+2.08	1997

Table 2. Average $\delta^{18}O$ values during 1800-1850 CE and post 1950 CE time slices, and the differences between them, in low-latitude ice cores from the Tibetan Plateau.

The truncated ice core climate record from Naimona'nyi does not imply that it stopped accumulating ice in the 1950s, but rather that any existing ice has been ablating for an undetermined length of time. Indeed, the glacier thinned by 2.21 meters between 2008 and 2013 (Tian et al., 2014), and its area decreased from 87 ± 8.7 km^2 in 1976 to 79.5 ± 4 km^2 in 2014 (Fig. 1B, Table S1). A combination of increasing air temperature and decreasing precipitation in the Himalayas and southern Tibetan Plateau is detrimental to the ice cover, as shown by the ablation on Naimona'nyi and other regional glaciers (Yao et al., 2012; Tian et al., 2014). The Dasuopu glacier was drilled 24 years ago and there have been no subsequent reports of its status. However, analysis of satellite imagery shows that the rates of elevation decrease of central

Himalayan glaciers, including Dasuopu, have increased from 2000 to 2019 (Supplementary Information in Hugonnet et al., 2021).

5. The consequences of continued warming on alpine glaciers, their climate records, and dependent communities

Over recent decades the diminishing surface area and thinning of many alpine tropical glaciers and the changes in the preservation of the climate signals recorded by stable isotopes of precipitation are driven by changes in climate on regional and global levels. Existing evidence indicates that rising temperatures, both atmospheric and oceanic, are globally pervasive and are primarily responsible for the diminishment of most of the tropical and mid-latitude high-elevation glaciers discussed here.

If the current global warming trend continues a large percentage of the world's low and middle latitude glaciers will lose a significant portion of their mass (Zemp et al., 2015) or even vanish completely by the end of this century. There is a consensus that the current glacier retreat is pervasive in the low- and mid-latitudes, and that an important driver is increasing temperatures (e.g., Thompson et al., 2011a; Yao et al., 2012; Schauweker et al., 2014, Zemp et al., 2015; Permana et al., 2019). From 2000 to 2019 there was a marked increase in aggregated temperature over glaciated areas of the world concomitant with glacier retreat and thinning, while precipitation increased only slightly (Hugonnet et al., 2021).

As glaciers retreat and even vanish the information they contain about past climatic and environmental changes will also disappear. Glaciers may regrow in the future if the current warming trend is eventually reversed, but the archives contained in their precursors are lost forever. The ice core records from the Peruvian Andes demonstrate that the glaciers below 6000 masl have been melting for ~40 years (Figs. 4, 6), while the records from inner Tropics near the Equator (Fig. 8) and from the western Himalayas (Fig. 10) show that glaciers in those regions have not accumulated ice for several decades and in fact have ablated from the summit surfaces. At the same time, temperature data from the higher altitudes of tropical Andes region (Vuille et al., 2015) and the western Tibetan Plateau (Thompson et al., 2018b) have trended upward since at least the mid-20th century. Just as alarmingly, model projections of future tropospheric temperature changes suggest that elevation dependent warming will increase over the next 100 years. Rates of temperature increase in the free atmosphere are predicted to be largest in the low latitudes, particularly at elevations above 6 km (Fig. 11) (Bradley et al., 2006) where many of the alpine glaciers studied by BPCRC-OSU are located. There are only a few sites at the very highest elevations that still preserve largely uncompromised ice core records; however, even these are most likely be at risk in the next few decades. The projected increasing rate of warming at higher altitudes will ensure that the climate records currently preserved in glaciers such as Huascarán and Guliya will soon begin to resemble those on Quelccaya and Naimona'nyi, and eventually those on Kilimanjaro and in Papua where the consequences of a rapidly changing climate have severely compromised the existing climate records. Thus, future innovative techniques and avenues of ice core research will only be possible for cores that have been drilled and are currently archived in freezer storage facilities around the world.

Many alpine glaciers are located close to human populations and thus, the impacts of climate changes on them will have both short- and long-term economic, social, and even cultural consequences. Not only are mountain glaciers important sources of stored water for regions that experience dry winters, but many indigenous societies in the Andes, the Himalayas, and East Africa regard them as sacred foci of belief systems in which they are considered to be homes of the gods or as sentient divine beings (Allison, 2015). For example, during the 2010 Papua drilling program, members of the BPCRC-OSU field team were made aware of the belief among many of the indigenous Amungme that the ice fields constituted the head of a divine being, and therefore cultural sensitivity was required to drill through "the skull of god". Although the disappearance of these glaciers in Papua will not adversely affect water resources in one of the wettest regions on Earth (Prentice and Hope, 2007), it can have profound impacts on spiritual and cultural identity.

The recent warming trends in land/ocean temperatures that are impacting the global cryosphere present challenges for the economies of many countries. The glacier contributions to water resources in South

America and South Asia are vital for agriculture and hydropower. In Peru almost half the population is concentrated in the rain shadow of the Andes between the arid coast and the mountains, and snow/ice meltwater constitutes 80% of the water resources here (Coudrain et al., 2005). Model projections of annual discharge for glaciated areas in the Cordillera Blanca indicate that under continued warming, the depletion of glacier ice will greatly increase dependence on the highly seasonal precipitation to supply streams and rivers (Chevallier et al., 2011). Glaciers in High Asia are recognized as an important water source in countries with rapidly expanding populations and the accompanying increases in water demands, particularly during droughts (Pritchard, 2017). These "drought buffers" are under stress, as glaciers in High Asia could lose 49 ± 7 to 64 ± 5% of their total mass by 2100 according to RCP projections (Kraaijenbrink et al., 2017). Even in the northwestern TP and in the Karakorum region where the surface area and total mass of glaciers has increased slightly in recent decades (Brun et al., 2017; Farinotti et al., 2020), new results from satellite archives indicate that this trend has reversed (Hugonnett et al., 2021).

6. Summary

The anticipated continuation of the reduction in surface area and thickness of many tropical alpine glaciers, and the concomitant melting that compromises the preservation of the climate histories they contain, are virtually certain according to the most recent IPCC (2014) predictions. These trends and their consequences have been demonstrated using in situ and satellite-borne observations and ice core-derived climate histories for high-elevation alpine glaciers in different geographical and climatological settings. Specific examples are drawn from the South American Andes, equatorial East Africa, Indonesia, northwestern Tibetan Plateau, and western Himalayas. Some glaciers are no longer preserving contemporary histories as their records are obliterated by percolation of melt water, while others are no longer accumulating mass are even being decapitated by the thinning of the surface ice.

The melting of these mountain glaciers poses potential threats to lives and livelihoods for nearby and downstream communities, many of which have growing populations. Due to the accumulation of meltwater, proglacial lakes are growing along the ice margins where they can become a source of destructive outburst floods, as was demonstrated in the case of communities to the west of the Quelccaya ice cap. Although the current melting of these alpine glaciers poses flood risks, eventually the volume of meltwater runoff will decline as glaciers in and near monsoon regions that serve as “drought buffers” shrink and result in water shortages, particularly during the dry season. Water shortages negatively affect local ecosystems, agriculture, power generation, sanitation, and personal consumption and can lead to negative impacts on food security, water quality, livelihoods, health and well-being, infrastructure, transportation, tourism, recreation, culture, and cultural identity (IPCC, 2019).

Expression of competing interests

The authors declare that they have no known competing financial interests or personal relationships that could have appeared to influence the work reported in this paper.

Acknowledgements

Funding for the 2016 and 2019 drilling projects on Huascarán and Quelccaya and the 2013 drilling project on Quelccaya was provided by the National Science Foundation (NSF) Paleoclimate Program awards RAPID AGS-1603377, and AGS 1805819 and AGS 0823586, respectively and by The Ohio State University (OSU). Prior field projects back to 1976 were funded by multiple awards from NSF, NOAA, and OSU. Funding for the photography of the Kilimanjaro glaciers was provided by OSU’s Climate, Water and Carbon Program, and NSF Award ATM-9910172. The Naimona’nyi program was funded by NSF Award ATM-0502476, and the Guliya program was funded by NSF Award P2C2-1502919. Funding for the Papua, Indonesia program was provided by NSF Award ATM-0823586. Support for ethnographic fieldwork in Phinaya in 2015 and 2016 was provided by a fellowship from the Johns Hopkins Environment, Energy, Sustainability & Health Institute. The authors wish to thank all the participants in the Quelccaya, Cordillera Blanca, Himalaya, Papua, and Kilimanjaro ice core drilling and surface sampling programs conducted by BPCRC-OSU since 1976. This is Byrd Polar and Climate Research Center contribution number C-1592.

References

Abram, N. J., McGregor, H. V., Gagan, M. K., Hantoro, W. S., Suwargadi, B. W., 2009. Oscillations in the southern extent of the Indo-Pacific Warm Pool during the mid-Holocene. *Quat. Sci. Rev.* 28, 2794-2803. doi: 10.1016/j.quascirev.2009.07.006.

Aggarwal, P. K., Romatschke, U., Araguas-Araguas, L., Belachew, D., Longstaffe, F. J., Berg, P., Schumacher, C., Funk, A., 2016. Proportions of convective and stratiform precipitation revealed in water isotope ratios. *Nat. Geosci.* **9**, 624-629. doi: 10.1038/NGEO02739.

Aguilar-Lome, J., Espinoza-Villar, R., Espinoza, J.-C., Rojas-Acuña, J., Willems, B. L., Leyva-Molina, W-M., 2019. Elevation-dependent warming of land surface temperatures in the Andes assessed using MODIS LST time series (2000-2017). *Int. J. App. Earth. Obs. Geoinf.* 77, 119-128. doi: 10.1016/j.jag.2018.12.013.

Albert, T., Klein, A., Kincaid, J. L., Huggel, C., Racoviteanu, A. E., Arnaud, Y., Silverio, W., Ceballos, J. L., 2014. Remote sensing of rapidly diminishing tropical glaciers in the northern Andes, in: Kargel, J. S., Leonard, G. J., Bishop, M. P., Kääb, A., Raup, B. H. (Eds.), *Global Land Ice Measurements from Space*. Springer, Berlin Heidelberg, pp. 609-638.

Allison, E. A., 2015. The spiritual significance of glaciers in an age of climate change. *WIREs Clim. Change* 6, 493-508. doi: 10.1002/wcc.354

Beniston, M., 2003. Climatic change in mountain regions: a review of possible impacts. *Clim. Change* 59, 5-31.

Bolch, T., Kulkarni, A., Kääb, A., Huggel, C., Paul, F., Cogley, J. G., Frey, H., Kargel, J. S., Fujita, K., Scheel, M., Bajracharya, S., Stoffel, M., 2012. The state and fate of Himalayan glaciers. *Science* 336, 310-314. doi: 10.1126/science.1215828.

Bradley, R. S., Keimig, F. T., Diaz, H. F., Hardy, D. R., 2009. Recent changes in freezing level heights in the Tropics with implications for the deglacierization of high mountain regions. *Geophys*. *Res*. *Lett*. 36, L17701. doi: 10.1029/2009GL037712.

Bradley, R. S., Vuille, M., Diaz, H. F., Vergara, W. 2006. Threats to water supplies in the tropical Andes. *Science* 312, 1755-1756. doi: 10.1126/science.1128087.

Brun, F., Berthier, E., Wagnon, P., Kääb, A., Treichler, D., 2017. A spatially resolved estimate of High Mountain Asia glacier mass balances from 2000 to 2016. *Nat*. *Geo*. 10, 668-673. doi: 10.1038/NGEO2999.

Cai, Z., Tian, L., 2016. Atmospheric controls on seasonal and interannual variations in the precipitation isotope in the East Asian Monsoon region, *J*. *Clim*. 29, 1339-1352. doi: 10.1175/JCLI-D-15-0363.1

Cauvy-Fraunié, S, Dangles, O, 2019. A global synthesis of biodiversity responses to glacier retreat. *Nat*. *Ec*. *and Evol*. 3, 1675-1685. doi: 10.1038/s41559-019-1042-8.

Chevallier, P., Pouyaud, B., Suarez, W., Condom, T., 2011. Climate change threats to environment in the tropical Andes: glaciers and water resources. *Region*. *Env*. *Change*. 11, 179-187. doi: 10.1007/s10113-010-0177-6.

Chiang, J. H., Sobel, A. H., 2002. Tropical tropospheric temperature variations caused by ENSO and their influence on the remote tropical climate. *J*. *Clim*. 15(18), 2616–2631. doi: 10.1175/1520-0442(2002)015<2616:TTTVCB>2.0.CO;2.

Christie, I., Fernandes, E., Messerli, H., Twining-Ward, L., 2013. Tourism in Africa: Harnessing tourism for growth and improved livelihoods (English). World Bank Group http://documents.worldbank.org/curated/en/723511468102894381/Tourism-in-Africa-harnessing-tourism-for-growth-and-improved-livelihoods.

Collier, E., Mölg, T., Sauter, T., 2018. Recent atmospheric variability at Kibo summit, Kilimanjaro, and its relation to climate mode activity. *J. Clim.* 31, 3875-3891. doi: 10.1175/JCLI-D-17-0551.s1.

Coudrain, A., Francou, B., Kundzewicz, Z. W., 2005. Glacier shrinkage in the Andes and the consequences for water resources-Editorial. *Hydrol. Sci. J.* 50, 925-932. doi:10.1623/hysj.2005.50.6.925.

Cullen, N. J., Sirguey, P., Mölg, T., Kaser, G., Winkler, M., Fitzsimons, S. J., 2013. A century of ice retreat on Kilimanjaro: the mapping reloaded. *Cryosphere* 7, 419-431. doi: 10.5194/tc-7-419-2013.

Duan, J., Esper, J., Büntgen, U., Li, L., Xoplaki, E., Zhang, H., Wang, L., Fang, Y., Luterbacher, J., 2017. Weakening of annual temperature cycle over the Tibetan Plateau since the 1870s. *Nat. Comm.* 8, 14008. doi: 10.1038/ncomms14008.

Dussaillant, I., Berthier, E., Brun, F., Masiokas, M., Hugonnet, R., Favier, V., Rabatel, A., Pitte, P., Ruiz, L., 2019. Two decades of glacier mass loss along the Andes. *Nat. Geosci.* 12, 802-808. doi: 10.1038/s41561-019-0432-5.

Farinotti, D., Immerzeel, W. W., de Kok, R. J., Quincey, D. J., Dehecq, A., 2020. Manifestations and mechanisms of the Karakorum glacier Anomaly. *Nat. Geosci.* 13, 8-16. doi: 10.1038/s41561-019-0513-5

Fu, Y., Liu, G., Wu, G., Yu, R., Xu, Y., Wang, Y., Li, R., Liu, Q., 2006. Tower mast of precipitation over the central Tibetan Plateau summer. *Geophys. Res. Lett.* 33, L05802. doi: 10.1029/2005GL024713.

Gadgil, S., Rajeevan, M., Francis, P. A., 2007. Monsoon variability: Links to major oscillations over the equatorial Pacific and Indian Oceans. *Curr. Sci.* 93, 182-194.

Garreaud, R., Vuille, M., Clement, A., 2003. The climate of the Altiplano: Observed current conditions and mechanisms of past changes, *Palaeogeogr*. *Palaeoclim*. *Palaeocl*., 194, 5–22. doi: 10.1016/S0031-0182(03)00269-4.

Hardy, D. R., Vuille, M., Bradley, R. S., 2003. Variability of snow accumulation and isotopic composition on Nevado Sajama, Bolivia. *J*. *Geophys*. *Res*. 108, 4693. doi: 10.1029/2003JD003623.

Hanshaw, M. N. and Bookhagen, B., 2014. Glacial area, lake areas, and snow lines from 1975 to 2012: status of the Cordillera Vilcanota, including the Quelccaya Ice Cap, northern central Andes, Peru. *Cryosphere* 8, 359-376. doi: 10.5194/tc-8-359-2014.

Hemp, A., 2006. Continuum or zonation? Altitudinal gradients in the forest vegetation of Mt. Kilimanjaro. Plant Ecol. 184, 27-42. doi: 10.1007/s11258-005-9049-4.

Herreros, J., Moreno, I., Taupin, J.-D., Ginot, P., De Angelis, M., Ledru, M.-P., Delachaux, F., Schotterer, U., 2009. Environmental records from temperature glacier ice on Nevado Coropuna saddle, southern Peru. *Adv*. *Geosci*. 22, 27-34. doi: 10.5194/adgeo-22-27-2009.

Hugonnet, R., McNabb, R., Berthier, E., Menounos, B., Nuth, C., Girod, L., Farinotti, D., Nuss, M., Dussaillant, I., Brun, F., Kääb, A., 2021. Accelerated global glacier mass loss in the early twenty-first century. *Nature* 592, 726-731. doi: 10.1038/s41586-021-03436-z.

Hurley, J. V., Vuille, M., Hardy, D. R., Burns, S. J., Thompson, L. G., 2015. Cold air incursions, $\delta^{18}O$ variability, and monsoon dynamics associated with snow days at Quelccaya Ice Cap, Peru. *J*. *Geophys*. *Res*. *Atmos*. 120, 7467-7487. doi:10.1002/2015JD023323.

Huss, M., Bookhagen, B., Huggel, C., Jacobsen, D., Bradley, R S., Clague, J. J., Vuille, M., Buytaert, W., Cayan, D. R., Greenwood, G., Mark, B. G., Milner, A. M., Weingartner, R., Winder, M., 2017. Toward mountains without permanent snow and ice. *Earth's Future* 5, 418-453. doi: 10.1002/2016EF000514.

Huss, M., Hock, R., 2018. Global-scale hydrological response to future glacier mass loss. *Nat. Clim. Change* 8, 135-140. doi: 10.1038/s41558-017-0049-xtps://d.

Imfeld, N., Sedlmeier, K., Gubler, S., Marrou, K. C., Davila, C. P., Huerta, A., Lavado-Casimiro, W., Rohrer, M., Scherrer, S. C., Shwierz, C., 2020. A combined view on precipitation and temperature climatology and trends in the southern Andes of Peru. *Int. J. Climatol.* 41, 679-698. doi: 10.1002/joc.6645.

IPCC, 2014. Climate Change 2014 Synthesis Report, in: Pachauri, R. K., Meyer, L. A. (Eds.), *Contribution of Working Groups I, II and III to the Fifth Assessment Report of the Intergovernmental Panel on Climate Change*. IPCC, Geneva, Switzerland, 151 pp.

IPCC, 2019. *IPCC Special Report on the Ocean and Cryosphere in a Changing Climate*, Pörtner, H.-O., Roberts, D.C., Masson-Delmotte, V., Zhai, P., Tignor, M., Poloczanska, E., Mintenbeck, K., Alegría, A., Nicolai, M., Okem, A., Petzold, J., Rama, B., Weyer, N. M. (Eds.), in press. https://www.ipcc.ch/srocc/cite-report/.

Kalnay, E., and 21 others, 1996. The NCEP/NCAR 40-year reanalysis project. *Bull. Am. Meteorol. Soc.* 77(3), 437-471. doi: 10.1175/1520-0477(1996)077<0437:TNYRP>2.0.CO;2.

Kehrwald, N. M., Thompson, L. G., Yao, T. D., Mosley-Thompson, E., Schotterer, U., Alfimov, V., Beer, J., Eikenberg, J., Davis, M. E., 2008. Mass loss on Himalayan glacier endangers water resources. *Geophys. Res. Lett.* 35, L22503. doi:10.1029/2008GL035556.

Kochtitzky, W. H., Edwards, B. E., Enderlin, E. M., Marino, J., Marinque, N., 2018. Improved estimates of glacier change rates at Nevado Coropuna Ice Cap, Peru. *J. Glaciol.* 64, 175-185. doi: 10.1017/jog.2018.2

Kraaijenbrink, P. D. A., Bierkens, M. F. P., Lutz, A. F., Immerzeel, W. W., 2017. Impact of a global temperature rise of 1.5 degrees Celsius on Asia's glaciers. *Nature* 549, 257-260. doi: 10.1038/nature23878.

Lamantia, K. A., 2018. Comparison of glacier loss on Qori Kalis, Peru and Mt. Kilimanjaro, Tanzania over the last decade using digital photogrammetry and stereo analysis. MSc Thesis, The Ohio State University, 85 pp.

Lenters, J. D., Cook, K. H., 1997. On the origin of the Bolivian High and related circulation features of the South American climate. *J. Atm. Sci.* 54, 656-677.

L'Heureux, M. L., Levine, A. F. Z., Newman, M., Ganter, C., Luo, J.-J., Tippett, M. K., Stockdale, T. N., 2020. ENSO prediction, in: McPhaden, M. J., Santoso, A., Cai, W. (Eds.), *El Niño Southern Oscillation in a Changing Climate, Geophysical Monograph 253*. Wiley, Washington DC., pp 227-246.

Maher, N., Matei, D., Milinski, S., Marotzke. J., 2018. ENSO change in climate projections: Forced response or internal variability? *Geophys. Res. Lett.* 45, 11,390–11,398. doi: 10.1029/2018GL079764.

Matthews, J. A., Briffa, K. R., 2005. The 'little ice age': re-evaluation of an evolving concept. *Geog. Ann.: Series A, Physical Geography* 87, 17-36. doi: 10.1111/j.0435-3676.2005.00242.x

Milner, A. M. and 16 others, 2017. Glacier shrinkage driving global changes in downstream systems. *Proc. Nat. Acad. Sci. (PNAS) USA* 114, 9770-9778. doi: 10.1073/pnas.1619807114

Mölg, T., Cullen, N. J., Hardy, D. R., Kaser, G., Nicholson, L., Prinz, R., Winkler, M., 2013. East African glacier loss and climate change: Corrections to the UNEP article "Africa without ice and snow". *Environ. Dev.* 6, 1-6. doi:10.1016/j.envdev.2013.02.001.

Mölg, T., Georges, C., Kaser, G., 2003. The contribution of increased incoming shortwave radiation to the retreat of the Rwenzori Glaciers, East Africa, during the 20th century. *Int. J. Climatol.* 23, 291-303. doi: 10.1002/joc.877.

Paegle, J. N., Mo, K.-C, 2002. Linkages between summer rainfall variability over South America and sea surface temperature anomalies. *J. Clim.* 15, 1389–1407. doi: 10.1175/1520-0442(2002)015<1389:LBSRVO>2.0.CO;2.

Pang, H., Hou, S., Zang, W., Wu, S., Jenk, T. M., Schwikowski, M., Jouzel, J., 2020. Temperature trends in the northwestern Tibetan Plateau constrained by ice core water isotopes over the past 7,000 years. *J. Geophys. Res.* 125, e2020JD032560. doi: 10.1029/2020JD032560.

Pang, Z., Kong, Y., Froehlich, K., Huang, T., Yuan, L., Li, Z., Wang, F., 2011. Processes affecting isotopes in precipitation of an arid region. *Tellus B* 63, 352-359. doi: 10.1111/j.1600-0889.2011.00532.x

Pepin N., and 20 others, 2015. Elevation-dependent warming in mountain regions of the world. *Nat. Clim. Change* 5, 424-430. doi: 10.1038/NCLIMATE2563.

Pepin, N. C., Deng, H., Zhang, H., Zhang, F., Kang, S., Yao, T., 2019. An examination of temperature trends at high elevations across the Tibetan Plateau: The use of MODIS LST to understand patterns of elevation- dependent warming. *J. Geophys. Res. Atmos.* 124, 5738–5756. doi: 10.1029/2018JD029798.

Permana, D. S., and 20 others, 2019. Disappearance of the Last Tropical Glaciers in the Western Pacific Warm Pool (Papua, Indonesia) appears imminent. *Proc. Nat. Acad. Sci. (PNAS) USA* 116(52), 26382-26388. doi: 10/1073/pnas.1822037116.

Permana, D. S., Thompson, L. G., Setyadi, G., 2016. Tropical west Pacific moisture dynamics and climate controls on rainfall isotopic ratios in southern Papua, Indonesia. J. Geophys. Res. 121, 2222-2245, doi: 10.1002/2015JD023893

Pollack, H., 2010. *A World Without Ice*, Avery, New York.

Prentice, M. L., Hope, G. S., 2007. Climate of Papua, in: Marshall, A. J., Beehler, B. M. (Eds.) *The Ecology of Papua: Part One*. Periplus, Singapore, pp. 177-195.

Prinz, R., Heller, A., Ladner, M., Nicholson, L. I., Kaser, G., 2018. Mapping the loss of Mt. Kenya's glaciers: An example of the challenges of satellite monitoring of very small glaciers. *Geosciences* 8, 174, doi: 10.3390/geosciences8050174.

Pritchard, H. D., 2017. Asia's glaciers are a regionally important buffer against drought. *Nature* 545, 169-174. doi: 10.1038/nature22062.

Qin, J., Yang, K., Liang, S., Guo, X., 2009. The altitudinal dependence of recent rapid warming over the Tibetan Plateau. *Clim. Change* 97, 321-327. doi: 10.1007/s10584-009-9733-9.

Rabatel, A., and 27 others, 2013. Current state of glaciers in the tropical Andes: a multi-century perspective on glacier evolution and climate change. *The Cryosphere* 7 (1), 81-102. doi:10.5194/tc-7-81-2013.

Racoviteanu, A. E., Arnaud, Y., Williams, M. W., Ornoñez, J., 2008. Decadal changes in glacier parameters in the Cordillera Blanca, Peru, derived from remote sensing. *J. Glaciol.* 54, 499-510. doi: 10.3189/002214308785836922.

Risi, C., Bony, S., Vimeux, F., 2008. Influence of convective processes on the isotopic composition ($\delta^{18}O$ and δD) of precipitation and water vapor in the tropics: 2. Physical interpretation of the amount effect. *J. Geophys. Res.* 113, D19306. doi: 10.1029/2008JD009943.

Rozanski, K., Araguás-Araguás, L., Gonfiantini, R., 1993. Isotopic patterns in modern global precipitation, in: Swarrt, P. K., Lohmann, K. C., McKenzie, J., Savin, S. (Eds.) *Climate Change in Continental Isotopic Records, Geophys. Mon. 78*, American Geophysical Union, Washington, pp. 1-36.

Samuels-Crow, K. E., Galewsky, J., Hardy, D. R., Sharp, Z. D., Worden, J., Braun, C., 2014. Upwind convective influences on the isotopic composition of atmospheric water vapor over the tropical Andes. *J. Geophys. Res.* 119, 7051-7063. doi: 10.1002/2014JD021487.

Schauwecker, S., Rohrer, M., Acuña, D., Cochachin, A., Dávila, L., Frey, H., Giráldez, C., Gómez, J., Huggel, C., Jacques-Coper, M., Loarte, E., Salzmann, N., Vuille, M., 2014. Climate trends and glacier retreat in the Cordillera Blanca, Peru, revisited. *Glob. Planet, Change* 119, 85-97, doi: 10.1016/j.gloplacha.2014.05.005.

Schauwecker, S., Rohrer, M., Huggel, C., Endries, J., Montoya, N., Neukom, R., Perry, B., Salzmann, N., Schwarb, M., Suarez, W., 2017. The freezing level in the tropical Andes, Peru: An indicator for present and future glacier extents. *J. Geophys. Res. Atmos.* 122, 5172-5189. doi: 10.1002/2016JD025943.

Schmidt, G. A., Bigg, G. R., Rohling, E. J., 1999. Global Seawater Oxygen-18 Database-v1.22. https://data.giss.nasa.gov/o18data/

Schmidt, G. A., LeGrande, A. N., Hoffmann, G., 2007. Water isotope expressions of intrinsic and forned variability in a coupled ocean-atmosphere model. J. Geophys. Res. 112, D10103. doi: 10.1029/JD007781.

Seehaus, T., Malz, P., Sommer, C., Lippl, S., Cochachin, A., Braun, M., 2019. Changes of the tropical glaciers throughout Peru between 2000 and 2016 – mass balance and area fluctuations. *The Cryosphere* 13, 2537–2556. doi: 10.5194/tc-13-2537-2019.

Shaman, J., Tziperman, E., 2004. The effect of ENSO on Tibetan Plateau snow depth: A stationary wave teleconnection mechanism and implications for the South Asian monsoons. *J. Clim.* 18, 2067-2079.

Stibal, M., Bradley, J. A., Edwards, A., Hotaling, S., Zawierucha, K., Rosvold, J., Lutz, S, Cameron, K. A., Mikucki, J. A., Kohler, T. J., Šabacka, M., Anesio, A. M., 2020. Glacial ecosystems are essential to understanding biodiversity responses to glacier retreat. *Nat. Ecol. Evol.* 4, 686–687. doi: 10.1038/s41559-020-1163-0.

Stuart-Smith, R. F., Roe, G. H., Li, S., Allen, M. R. 2021. Increased outburst flood hazard from Lake Palcacocha due to human-induced glacier retreat. *Nat. Geosci.* 14, 85-90. doi: 10.1038/s41561-021-00686-4.

Taylor, R. G., Mileham, L., Tindimugaya, C., Majugu, A., Muwanga, A., Nakileza, B., 2006. Recent glacial recession in the Ruwenzori Mountains of East Africa due to rising air temperature. *Geophys. Res. Lett.* 33, L10402. doi: 10.1029/2006GL025962.

Thompson, L.G., 1978. Ice core studies from Mt. Kenya, Africa, and their relationship to other tropical ice core studies, in: Allison, I. (Ed.), *Sea level, ice and climatic change: Proceedings of the XVII Assembly of the IUGG Canberra Symposium*, December, 1979, IAHS Publ. no. 131, pp. 55-62.

Thompson, L. G., Brecher, H. H. Mosley-Thompson, E. Hardy, D. R., Mark, B. G., 2009. Glacier loss on Kilimanjaro continues unabated. *Proc. Nat. Acad. Sci. (PNAS) USA* 106, 19770-19775. doi: 10.1073/pnas.0906029106.

Thompson, L. G., Davis, M. E., Mosley-Thompson, E., Beaudon, E., Porter, S. E., Kutuzov, S., Lin, P.-N., Mikhalenko, V. N., Mountain, K. R., 2017. Impacts of recent warming and the 2015/16 El Niño on tropical Peruvian ice fields. *J. Geophys. Res. Atmos.* 122. doi: 10.1002/2017JD026592.

Thompson, L.G., Davis, M. E., Mosley-Thompson, E., Sowers, T. A., Henderson, K. A., Zagorodnov, V. S., Lin, P.-N., Mikhalenko, V. N., Campen, R. K., Bolzan, J. F., Cole-Dai, J., Francou, B., 1998. A 25,000 year tropical climate history from Bolivian ice cores. *Science,* 282(5295), 1858-1864. doi: 10.1126/science.282.5395.1858.

Thompson, L. G., Mosley-Thompson, E., Brecher, H., Davis, M., León, B., Les, D., Lin, P.-N., Mashiotta, T., Mountain, K., 2006. Abrupt tropical climate change: past and present. *Proc. Nat. Acad. Sci. (PNAS) USA* 103(28), 10536-10543. doi: 10.1073/pnas.0603900103.

Thompson, L.G., Mosley-Thompson, E., Dansgaard, W., Grootes, P. M., 1986. The "Little Ice Age" as recorded in the stratigraphy of the tropical Quelccaya ice cap. *Science*, 234, 361-364. doi: 10.1126/science.234.4774.361.

Thompson, L.G., Mosley-Thompson, E., Davis, M. E., Lin, P.-N., Henderson, K. A., Cole-Dai, J., Bolzan, J. F., Liu, K-b., 1995. Late Glacial Stage and Holocene tropical ice core records from Huascarán, Peru. Science 269, 46-50. doi: 10.1126/science.269.5220.46.

Thompson, L. G., Mosley-Thompson, E., Davis, M. E., Henderson, K. A., Brecher, H. H., Zagorodnov, V. S., Mashiotta, T. A., Lin, P.-N., Mikhalenko, V. N., Hardy, D. R., Beer, J., 2002. Kilimanjaro ice core records: Evidence of Holocene climate change in tropical Africa. *Science* 298, 589-593. doi: 10.1126/science.1073198.

Thompson, L. G., Mosley-Thompson, E., Davis, M. E., Brecher, H. H., 2011a. Tropical glaciers, recorders and indicators of climate change, are disappearing globally. *Ann*. *Glaciol*. 52, 23-34. doi: 10.3189/172756411799096231.

Thompson, L. G., Mosley-Thompson, E., Davis, M. E. Mountain, K., 2011b. A paleoclimatic perspective on the 21st-century glacier loss on Kilimanjaro, Tanzania. *Ann*. *Glaciol*. 52, 60-68. doi: 10.3189/172756411799096349.

Thompson, L. G., Mosley-Thompson, E., Davis, M. E., Zagorodnov, V. S., Howat, I. M., Mikhalenko, V. N., Lin, P.-N., 2013. Annually resolved ice core records of tropical climate variability over the past ~1800 years. *Science* 340, 945-950. doi: 10.1126/science.1234210.

Thompson L. G., Mosley-Thompson, E., Davis, M. E., Porter, S. E., Kenny, D. V., Lin, P.-N., 2018a. Global-scale abrupt climate events and black swans. An ice-core-derived palaeoclimate perspective from Earth's highest mountains, in: Pant, N. C., Ravindra, R., Srivastava, R., Thompson, L. G. (Eds.), *The Himalayan Cryosphere: Past and Present*. Geological Society, London, Special Publications 462, pp. 7-22. doi: 10.1144/SP462.6.

Thompson, L. G., Yao, T., Davis, M. E., Mosley-Thompson, E., Wu, G., Porter, S. E., Xu, B., Lin, P.-N., Wang, N., Beaudon, E., Duan, K., Sierra-Hernández, M. R., Kenny, D. V., 2018b. Ice core records of climate variability on the Third Pole with emphasis on the Guliya ice cap, western Kunlun Mountains. *Quat. Sci. Rev.* 188, 1-14. doi: 10.1016/j.quascirev.2018.03.003.

Thompson, L. G., Yao, T., Mosley-Thompson, E., Davis, M. E., Henderson, K. A., Lin, P.-N., 2000. A high-resolution millennial record of the South Asian monsoon from Himalayan ice cores. *Science* 289, 1916-1919. doi: 10.1126/science.289.5486.1916.

Tian, L., Zong, J., Yao, T., Ma, L., Pu, J., Zhu, D., 2014. Direct measurement of glacier thinning on the southern Tibetan Plateau (Gurenhekou, Kangwure, and Naimona'Nyi glaciers). *J. Glaciol.* 60, 879-888. doi: 10.3189/2014JoG14J022 879.

Veettil, B. K., Bremer, U. F., de Souza, S. F., Maier, E. L. B., Simões, J. C., 2016. Influence of ENSO and PDO on mountain glaciers in the outer tropics: case studies in Bolivia. *Theor. Appl. Climatol.* 125, 757-768. doi: 10.1007/s00704-015-1545-4.

Veettil, B. K., Simões, J. C., 2019. The 2015/15 El Niño-related glacier changes in the tropical Andes. *Front. Earth. Sci.* 13, 422-429. doi: 10.1007/s11707-018-0738-4.

Veettil, B. K., Wang, S., De Souza, S. F., Bremer, U. F., Simões, J. C., 2017. Glacier monitoring and glacier-climate interactions in the tropical Andes: A review. *J. S. Am. Earth Sci.* 77, 218-246. doi: 10.1016/j.jsames.2017.04.009.

Vuille, M., Bradley, R. S., Werner, M., Healy, R., Keimig, F., 2003. Modeling $\delta^{18}O$ in precipitation over the tropical Americas: 1. Interannual variability and climatic controls. *J. Geophys. Res.* 108, 4174. doi:10.1029/2001JD002038.

Vuille, M., Franquist, E., Garreaud, R., Casimiro, W. S. L., Cáceres, B., 2015. Impact of the global warming hiatus on Andean temperature. *J. Geophys. Res.* 120, 3745-3757. doi: 10.1002/2015JD023126.

Vuille, M., Kaser, G., Juen, I., 2008. Glacier mass balance variability in the Cordillera Blanca, Peru and its relationship with climate and large-scale circulation. *Glob. Planet. Change* 62, 14–28. doi: 10.1016/j.gloplacha.2007.11.003.

Vuille, M., Werner, M., Bradley, R. S., Keimig, F., 2005. Stable isotopes in precipitation in the Asian monsoon region. *J. Geophys. Res.* 110, D23108. doi: 10.1029/2005JD006022.

Yao, T., Masson-Delmotte, V., Gao, J., Yu, W. S., Yang, X. X., Risi, C., Sturm, C., Werner, M., Zhao, H. B., He, Y., Ren, W., Tian, L. D., Shi, C. M., Hou, S. G., 2013. A review of climatic controls on δ^{18}O in precipitation over the Tibetan Plateau: observations and simulations. *Rev. Geophys.* 51, 525e548. doi: 10.1002/rog.20023.

Yao, T. D., Thompson, L., Yang, W., Yu, W., Gao, Y., Guo, X., Yang, X., Duan, K., Zhao, H., Xu, B., Pu, J., Lu, A., Xiang, Y., Kattel, D. B., Joswiak, D., 2012. Different glacier status with atmospheric circulations in Tibetan Plateau and surroundings. *Nat. Clim. Change* 2, 663-667. doi: 10.1038/NCLIMATE1580.

Yao, T., 37 others, 2019. Recent Third Pole's rapid warming accompanies cryospheric melt and water cycle intensification and interactions between monsoon and environment: Multidisciplinary approach with observations, modeling, and analysis. *Bull. Amer. Meteorol. Soc.* 100(3). doi: 10.1175/BAMS-D-17-0057.1.

Yarleque, C., Vuille, M., Hardy, D. R., Timm, O. E., De la Cruz, J., Ramos, H., Rabatel, A., 2018. Projections of the future disappearance of the Quelccaya Ice Cap in the Central Andes. *Sci. Rep.* 8, 15564. doi: 10.1038/s41598-018-33698-z.

Yu, W., Yao, T., Thompson, L. G., Jouzel, J., Zhao, H., Xu, B., Jing, Z., Wang, N., Wu, G., Ma, Y., Gao, J., Yang, X., Zhang, J., Qu, D., 2020. Temperature signals of ice core and speleothem isotopic records from Asian monsoon region as indicated by precipitation δ^{18}O. *Earth Planet Sci. Lett.* 116665. doi: 10.1016/j.epsl.2020.116665.

Zemp, M., 38 others, 2015. Historically unprecedented global glacier decline in the early 21st century. *J. Glaciol*. 61, 745-762. doi: 10.3189/2015JoG15J017.

Figure captions

Figure 1. The surface area changes from the late 20th to the early 21st centuries are shown for: (A) The glaciers on Kilimanjaro, East Equatorial Africa (3ºS); (B) Naimona'nyi glacier, western Himalayas (30ºN); (C) Quelccaya ice cap, Andes of southern Peru (14.5ºS), and (D) the glaciers near Puncak Jaya, Indonesia (New Guinea) (4ºS). The global map shows areas of ice retreat (red shading). The locations of additional low-latitude glaciers discussed in the text are also shown. Ice retreat regions are from the National Snow and Ice Data Center (https://nsidc.org/glims/glaciermelt).

Figure 2. Relief map of western South America and the outer tropical Andes showing the locations of the glaciers discussed in the text (https://iridl.ldeo.columbia.edu/SOURCES/.NOAA/.NGDC/.GLOBE/.topo/). The glaciers in the Cordillera Blanca in northern Peru from which shallow cores have been obtained are shown in the inset (Google Earth Pro). The black dashed line traces the elevation cross-section in Fig. 4 from Huascarán southward through the drill sites to Sajama in Bolivia (source: Google Earth Pro).

Figure 3. Photo of the western margin of Nevado Huascarán taken in austral winter 2019 shows fresh rock exposed by the retreating ice, the edge of which is outlined by the white solid line. The dark area below the exposed rock, outlined by the white dashed line, is vegetation which marks the ice extent in 1970. Photo by L. G. Thompson.

Figure 4. $\delta^{18}O$ profiles from five ice cores drilled in the Peruvian Andes and on the Altiplano of Bolivia, arranged from north to south. The $\delta^{18}O$ sample data are illustrated in two time slices, 1800 to 1850 CE and 1950 CE to the top of each record, and the mean $\delta^{18}O$ values for these two periods are shown for each record in Table 1. Timescale development is discussed for: Huascarán in Thompson et al. (1995) (and updated with $\delta^{18}O$ data from a core drilled in 2019), for Quelccaya in Thompson et al. (1986; 2013), for Coropuna in Thompson et al. (2018a), and for Sajama in Thompson et al. (1998). The elevation profile below (Google Earth Pro) shows the topography from north to south (black dashed line in Fig. 2) and the relative elevations of the glaciers in this section of the outer tropical Andes. The year of drilling is shown at the top of each core. The analytical error of $\delta^{18}O$ is ±0.2‰.

Figure 5. Profiles of $\delta^{18}O$ from cores drilled on glaciers throughout the Cordillera Blanca, arranged from north (left) to south (right). The elevation profile (below) shows the north to south topography (yellow dashed line in Fig. 2, inset) and relative elevations of the glaciers in this section of the Cordillera Blanca. Except for Huascarán, these cores were drilled at elevations below 5500 masl and their $\delta^{18}O$ records show smoothing of the annual signal due to water percolation through the firn that confirms melting was well underway at high elevations at the time the cores were drilled. The year of drilling is shown at the top of each core. The analytical error of $\delta^{18}O$ is ±0.2‰.

Figure 6. (A) Profiles of $\delta^{18}O$ from shallow cores drilled on the summit of the Quelccaya ice cap from 1976 to 2018 illustrating the attenuation of the seasonal isotopic variations toward the present associated with warming and

percolation of meltwater through the firn. The month and year of drilling is shown at the top of each core. The analytical error of $\delta^{18}O$ is ±0.2‰. (B) Reanalysis temperatures at 500 mb in the vicinity of the Quelccaya ice cap from 1975/75 to 2019/20 (thermal year averages). The strong El Niños are marked by red closed circles, and the temperature at which intense $\delta^{18}O$ attenuation is first observed (1979 profile in (A)) is shown by a broken line. Temperature trend lines and their slopes from 1975/76 to 1999/2000 and from 1999/2000 to 2019/2020 are shown as red lines and text. The years of the Qori Kalis and Phaco GLOFs are shown. Data are from NOAA NCEP-NCAR CDAS-1 MONTHLY Intrinsic Pressure Level Temperature (Kalnay et al., 1996).

Figure 7. Google Earth image of the region west of Quelccaya ice cap in southern Peru shows the path of water and debris from a lake outburst that struck the community of Phaco in December 2007. The lake formed as Quelccaya ice melted and water pooled. The outburst was caused by what community leaders concluded was a large piece of ice from the ice margin that fell into the lake. The Qori Kalis glacier and its proglacial lake is shown north of the Phaco GLOF source.

Figure 8. $\delta^{18}O$ profiles from two equatorial ice fields. (A) $\delta^{18}O$ record from the 10-meter thick Furtwängler glacier in the Kibo crater, Kilimanjaro; (B) $\delta^{18}O$ record from the East Northwall Firn ice field near Puncak Jaya, Papua Indonesia. The locations of the two sites are shown on the global map below. The timescale for FWG core is discussed in Thompson et al. (2002), and the dating of the East Northwall Firn core is discussed in Permana et al. (2019). The analytical error of $\delta^{18}O$ is ±0.2‰.

Figure 9. Relief map of the Third Pole showing the locations of the Guliya ice cap and the Dasuopu and Naimona'nyi glaciers from which ice cores have been retrieved, along with the trajectories of the primary air masses and the major rivers of South Asia. The black dashed line traces the elevation cross-section (top) from the Tarim Basin north of Guliya, through the drill sites and to the south slope of the Himalayas southeast of Dasuopu (source: Google Earth Pro). Relief map source: https://iridl.ldeo.columbia.edu/SOURCES/.NOAA/.NGDC/.GLOBE/.topo/

Figure 10. (A) $\delta^{18}O$ profiles from three ice cores from the Tibetan Plateau and the Himalayas, arranged from north to south. The $\delta^{18}O$ sample data are illustrated in two time slices, 1800 to 1850 CE and 1950 CE to the top of each record, and the mean $\delta^{18}O$ values for the two periods from each record are shown in Table 1. Timescale development is discussed for Guliya in Thompson et al. (2018b), for Dasuopu in Thompson et al. (2000) and for Naimona'nyi in Supplement Section 1. The year of drilling is shown at the top of each core. The analytical error of $\delta^{18}O$ is ±0.2‰. (B). Annual averages of $\delta^{18}O$ from the three ice core records from 1901 to the top. Note that Naimona'nyi is truncated at 1957 CE, although the core was drilled in 2006 (marked by red arrow on x-axis).

Figure 11. Projected zonal annual temperature changes with height in the atmosphere between 2000-2009 and 2090-2099. The multi-model mean for RCP 8.5 was calculated by KNMI Climate Explorer using CMIP5 data from https://esgf-node.llnl.gov/search/cmip5/. Latitudes and altitudes are shown for the tropical and mid-latitude alpine glaciers from which ice cores discussed in the paper were drilled. "C.B. sites" indicates the alpine glaciers (Hualcán, Pucahirca, Copap, and Caullaraju) drilled in the Cordillera Blanca, in addition to Huascarán (see Fig. 2, inset).

Supplemental Information

S1. Timescale development for Naimona'nyi ice core record

The Naimona'nyi and Dasuopu glaciers receive most precipitation from both the Indian summer monsoon and the continental westerlies. However, because it is located in the western Himalayas and further inland away from the monsoon source, the westerly to monsoon moisture ratio is higher for Naimona'nyi. In addition, in 1997 Dasuopu had a ~50 meter firn layer, while the Naimona'nyi glacier currently lacks firn and is composed of ice to the surface, which has been ablating for an undetermined number of years. Although Dasuopu contains well defined wet summer/dry winter seasonal oscillations in $\delta^{18}O$, the seasonality on Naimona'nyi is more difficult to detect.

Despite these difficulties, the $\delta^{18}O$ profiles between these two Himalayan glaciers can be matched using AnalySeries software (Paillard et al., 1996) (Fig. S1). We know that the lack of a 1962/63 beta radioactivity horizon (from early 1960s Soviet bomb tests in the Arctic) and the lack of a 1950s ^{36}Cl signal from marine nuclear tests in the South Pacific indicate that the top of the Naimona'nyi core is no more recent than the late 1950s (Kehrwald et al., 2008). Since the 1962/63 horizon occurs in the Dasuopu core at 42 meters, we disregarded that part of the Dasuopu core during the AnalySeries match with the Naimona'nyi $\delta^{18}O$ data. With the depth of each Naimona'nyi $\delta^{18}O$ value matched to its corresponding depth in the Dasuopu record, the annual timescale from the latter can be transferred to the former.

Figure S1. AnalySeries match between $\delta^{18}O$ from the Naimona'nyi ice core (red curve) and smoothed (11-sample running means) Dasuopu ice core $\delta^{18}O$ data. The year (CE) is shown every five meters on the Dasuopu depth scale. The linear correlation between the curves is +0.65 ($p < 0.001$).

S2. Estimation of glacier surface area

S2.1. Imagery Selection

To minimize uncertainty in our area estimates, we chose to analyze only selected images from the entire archive available through the USGS's Global Visualization Viewer (GloVis). Because GloVis allows the analyst to step through every image available for a specific location, several essential advantages are achieved. First, because the viewer's cursor can be placed on a specific geographic reference point, images that are poorly geolocated, especially early in the Landsat time series, can be excluded from the analysis. Second, time periods with few acquisitions or acquisitions not useful for this particular study such as ascending scenes (essentially night acquisitions in the mid-latitudes) can also be identified. Third, by looking at multiple images per year in succession, it becomes fairly clear by inspection which images have the least cloud, snow cover, and the most solar illumination to limit shadows over the area's terrain and ice-covered areas. And lastly, by limiting the Landsat images selected for detailed analysis, it then becomes clearer which periodic images over the Landsat time frame allow ice area changes to be determined for a specific ice-remnant area.

Some ancillary considerations include: 1) minimizing scan-line errors that can negatively impact the classification scheme, most common in the limited number of Landsat 1-3 MSS scenes; 2) using Landsat-7 Scan Line Corrector off (SLC-off) imagery only when necessary but considering them especially when the target area is in the complete center swath; 3) accepting that not all snow can be assessed and excluded visually from even the 'best images' available; and 4) in contrast, accepting that the spectral resolution of Landsat sensors means that ice areas in full shadow cannot be assessed by the classification scheme. In essence, the last two factors 'add to' and 'subtract from' the resulting ice estimates. Similar impacts on area estimates result, respectively, from the presence of pro-glacial lakes, sometimes frozen, and debris-covered glacial outlets from some of the larger ice caps and cordillera.

S2.2 Analysis Approach

After all the 'likely' images are ordered from the United States Geological Survey (USGS), they are then downloaded and imported into PCI Geomatica Focus (https://www.pcigeomatics.com). The images are then stacked chronologically and a more detailed check for snow cover and cloud patches is conducted. Small geolocation errors may also be noted and, if insignificant, tolerated for the ice area analyses. Due to the reduced availability of imagery in the 1970s and 1980s, lower quality Multi Spectral Scanner (MSS) and Thematic Mapper (TM) images may be used to establish 'overall ice extent' even though they are more likely to include snow cover on and near actual glacial ice areas. By examining each possible image relative to those before and after, imagery with excessive snow cover can be excluded from further analysis.

Once the imagery series is selected, a region that encompasses the ice areas is subset or clipped from each full image and analyzed using an unsupervised classification algorithm in Focus using the short-wave infrared, near infrared, red, and green data channels. There are multiple analysis options within Focus but our process always used the 'IsoData' option with '16 Clusters'. Once the algorithm has been run, the classification result is saved. The subsequent Post Classification Analysis then requires the analyst to select the classes within the 16 outputs for aggregation as 'ice' and 'non-ice' portions of the image subset. By flickering the classification output relative to the underlying imagery, it is usually quite clear which classes belong in each category. This becomes more difficult if there are clouds or snow in any portion of the area as they tend to classify independently of the actual ice area. For more complex terrain such as Naimona'nyi, multiple subsets are necessary to derive the full ice area estimate. In particular, debris-covered outlet glaciers such as a large north-flowing one at this location cannot be assessed by this technique. For simpler terrain such as Puncak Jaya where all the remaining ice is exposed along a high ridge line, a single image subset is sufficient.

S2.3. Uncertainty Estimate

As summarized by Paul et al. (2015), there is inherent uncertainty within the results of the process outlined above and there are essentially no independent measurements that can be made to fully constrain area estimate uncertainties. Because our goal was to show ice area trends for each location through time, we elected to use a 10% uncertainty for any MSS-based estimate and 5% uncertainty for any TM, Enhanced Thematic Mapper Plus (ETM+), or Operational Land Imager (OLI) based ice area estimate. Although obviously expedient, this conservative area error value, scaling with the resulting ice area estimate, enables consistent comparisons over the full range of Landsat imagery available for each location. For areas with more imagery, the trends are unambiguous but further imagery through time will be required to better constrain the trends for areas with fewer high-quality images available for analysis.

Table S1. Landsat surface area measurements of tropical glaciers

Site	Date	Landsat	Sensor/ Resolution	Path Row	Area Estimate (km^2)	Error Estimate (km^2)
Kibo Crater Kilimanjaro	Aug 17, 1986	5	TM/30	168 062	5.56	0.28
	Aug 21, 2002	7	ETM+/30	168 062	3.09	0.15
	July 15, 2009	5	TM/30	168 062	1.88	0.09
	Sept 7, 2017	8	OLI/30	168 062	1.63	0.08
Naimona'nyi	Dec 6, 1976	2	MSS/60	155 039	87.0[#]	8.70
	Oct 13, 1998	5	TM/30	144 039	82.2	4.11
	Oct 13, 2001	7	ETM+/30	144 039	80.0	4.00
	Sept 9, 2014	8	OLI/30	144 039	79.50	3.98
Quelccaya	Oct 28, 1975	2	MSS 60	003 070	77.25[&]	7.72
	Aug 26, 1985	5	MSS 60	003 070	65.11	6.51
	Aug 2, 1988	5	TM 30	003 070	58.09	2.90
	July 26, 1991	5	TM 30	003 070	57.43	1.15
	Oct 9, 1995	5	TM 30	003 070	55.63	2.78
	Nov 21, 1999	5	TM 30	003 070	51.99	1.04
	Aug 17, 2005	5	TM 30	003 070	47.07	0.94
	Sept 16, 2010	5	TM 30	003 070	44.63	0.89
	Aug 7, 2013	8	OLI 30	003 070	45.80	0.92
	Oct 5, 2017	8	OLI 30	003 070	42.34	0.85
	Oct 11, 2019	8	OLI 30	003 070	41.41	0.83
Glaciers near Puncak Jaya	Aug 8, 1980	4	MSS 60	110 063	6.34	0.63
	Sept 8, 1982	2	MSS 60	103 063	6.07	0.61
	Nov 3, 1988	5	TM 30	103 063	4.67	0.23
	Nov 17, 1993	5	TM 30	103 063	3.36	0.17
	Oct 9, 1999	5	TM 30	103 063	2.74	0.14
	Oct 14, 2004	5	TM 30	103 063	1.88	0.09
	Oct 28, 2009	5	TM 30	103 063	1.29	0.06
	Oct 13, 2015	8	OLI 30	103 063	0.56	0.03
	Mar 11, 2018	8	OLI 30	103 063	0.47	0.02

[#]Area value from Ye et al. (2006), Table 5

[&]Composite image with one from Jul 29, 1975 (002 070)

S3. A local account of a GLOF in 2007 in Phaco, near the Quelccaya ice cap in southern Peru

The following ethnographic vignette introduces briefly how the complexity of the retreat of the Quelccaya ice cap unfolds in everyday life in Phinaya, an Andean village located near it. Figure 7 in the main text shows the locations described in these accounts.

The night the flood happened, almost everyone was out of Phaco, one of the most remote sub-sectors of the Phinaya Andean village, attending a community meeting in central Phinaya. Communal meetings play a key role in the social life in rural Andean communities and, as attendees tend to engage actively in the discussions, they frequently extend until late at night. This was not an exception that day.

Among the few who stayed in Phaco that night was *Luisa*, a neighbor from Phaco, who witnessed that everything started by midnight with an intense sound: *Brrrr, brrrr, brrrr brooooom*, as she later told *Domingo*, one of her neighbors in Phaco. At that point, she could not determine that all that noise was linked to a flood that was about to change her life forever. *How could she know that a landslide was coming to Phaco, anyway? Domingo* continues. *Can you imagine all that noise? Brrr brrrrr brrr, brooooom… and then the water, the mud, and the stones…. Plajjj, plajjj, plajjjj…. What could it be? Where was all that water coming out from? We didn't even know that there was a lake up there!* He confronts us.

As we can learn from *Domingo's* testimony, glacial lakes remain typically unknown for the locals until they flood. When those who spent the night in central Phinaya returned to Phaco early the next morning, they also could not understand what was going on. The landscape they were used to see every day was suddenly almost unrecognizable. *Greywater was coming out from all the streams and canals – that at that point were almost destroyed—, and the whole grasslands were covered with a grey mud that almost looked like lava, Domingo* remembers. Furthermore, their grazing infrastructure, which they had been patiently implementing and expanding during the last decades, was destroyed as the force of the water pulled it out of the ground, broke it in parts, and dragged the pieces very far away into the valley.

Among the most affected by this flood were *Maria*, one of the few who stayed in Phaco that night, and *Luis*, her husband. The flood changed their lives dramatically. It affected their livelihoods, as it destroyed most of the grass in their lands that still, more than ten years after, have not fully recovered. As *Javier*, another local herder from Phaco explained to us in detail:

> *The flood deposited a large amount of grey sand to their land, and a strong rotting smell started coming out of it after a few days but lasted for weeks. This killed the grass that still today has only been able to regrow in specific small patches in their land. You can still see today a big grey colored area in their land, the grey sand that came with the flood and doesn't let the grass grow anymore. A short time after the flood, Luis and his wife just ended selling their cattle; and later, they decided to rent their land and move to Sicuani (a small city located 4 hours away from Phinaya). Since they had moved, they have only come to visit and check their land a very few times."*

Furthermore, as Javier also highlights, the flood also affected *Maria* emotionally: *Maria was always* asustada *[frightened] after [the flood]. What might she had felt? Total fear, right?*

The community president at the time of the flood also provides some insights into this issue. As we were told by him, besides understanding the causes of the flood, one of their biggest concerns after this event was to verify that the community was not in danger of being affected by a larger flood in the following days. For that reason, they sent letters and visited different branches of the National Institute of Civil Defense (INDECI), the official body in charge of the response to disaster events in Peru, requesting that an expert team to evaluate the causes of these events and to investigate if more of these events could not occur in the future. However, they never received a response.

Before the flood, locals in Phaco were not used to visiting the land near the ice cap. It was only after weeks of not receiving a response from INDECI that the community organized an expedition to visit the base of the glacier and document the situation themselves. *Domingo*, who was part of the delegation who visited the lake, explained this in detail: *We are not used getting very close to the ice cap. What for? There is no grass there. Before the flood, we sometimes approached that area only if a llama had escaped, but never that close to the ice cap. That's why none of us knew that there was a lake there until then*. The expedition, however, allowed them to discover that there was a new lake at the foot of the Quelccaya. As *Domingo* remembers, that day they saw pieces of ice floating on the lake, which allowed them to understand that a big piece of ice had fallen into the lake and made it overflow.

Fortunately, there have been no floods in Phaco since that event. However, after the flood, local lakes and glacier retreat, have become a topic of major concern for the locals, and now are frequently raised in the community meeting debates.

References

Kehrwald, N. M., Thompson, L. G., Yao, T. D., Mosley-Thompson, E., Schotterer, U., Alfimov, V., Beer, J., Eikenberg, J., Davis, M. E., 2008. Mass loss on Himalayan glacier endangers water resources. *Geophys. Res. Lett.* 35, L22503. doi:10.1029/2008GL035556.

Paillard, D., Labeyrie, L., You, P., 1996. Analyseries 1.0: A Macintosh software for the analysis of geographical time-series. *Eos* **77**, 379.

Paul, F., et al., 2015. The glaciers climate change initiative: Methods for creating glacier area, elevation change and velocity products. *Remote Sens. Environ.* 162, 408-426. doi:/10.1016/j.rse.2013.07.043.

Ye, Q., Yao, T., Kang, S., Chen F., Wang, J., 2006. Glacier variations in the Naimona'nyi region, western Himalaya, in the last three decades. *Ann. Glaciol.* 43, 385–389. doi: 10.3189/172756406781812032.

Figure 1

Click here to access/download;Figure;Figure 1.jpg

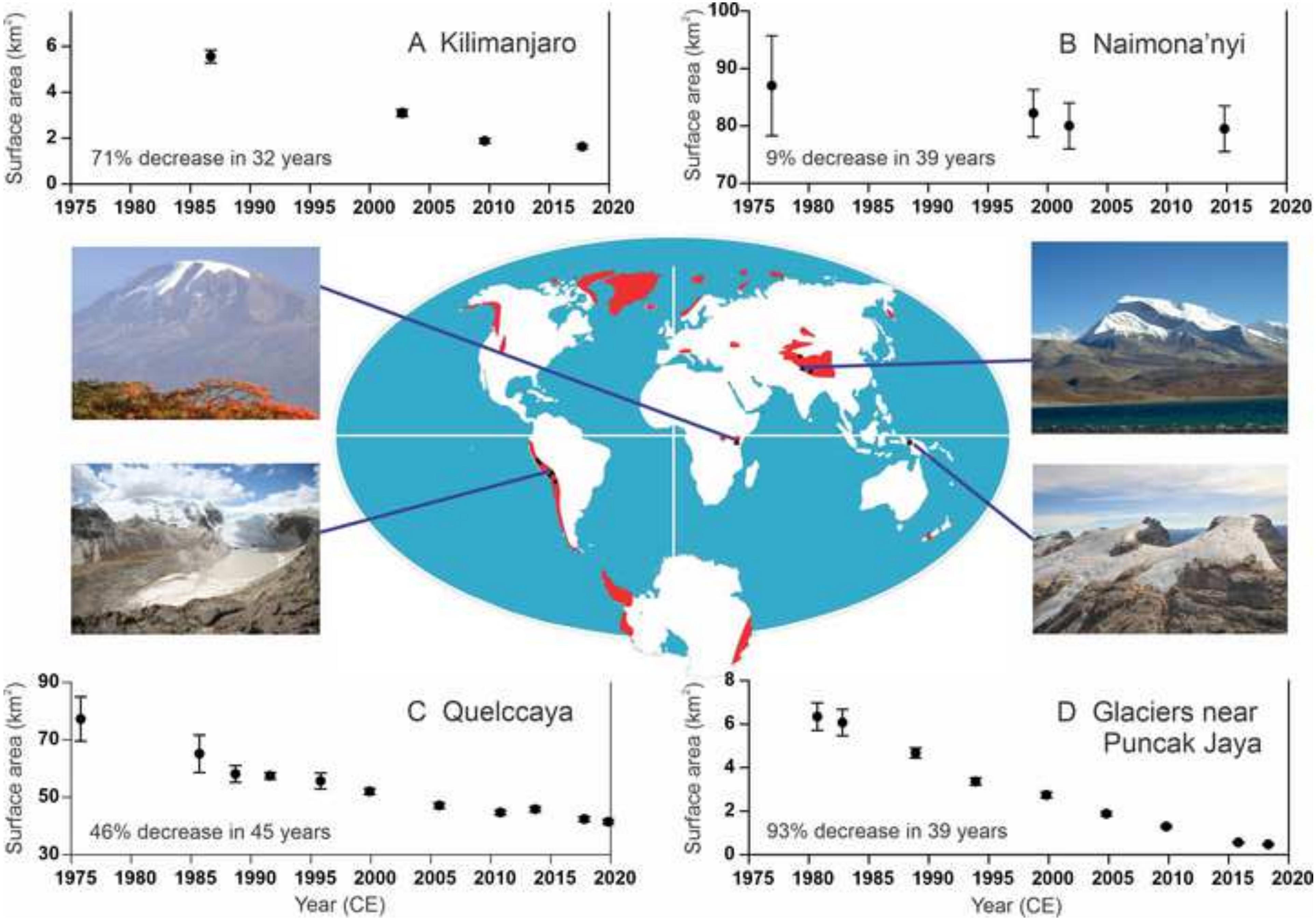

Figure 2

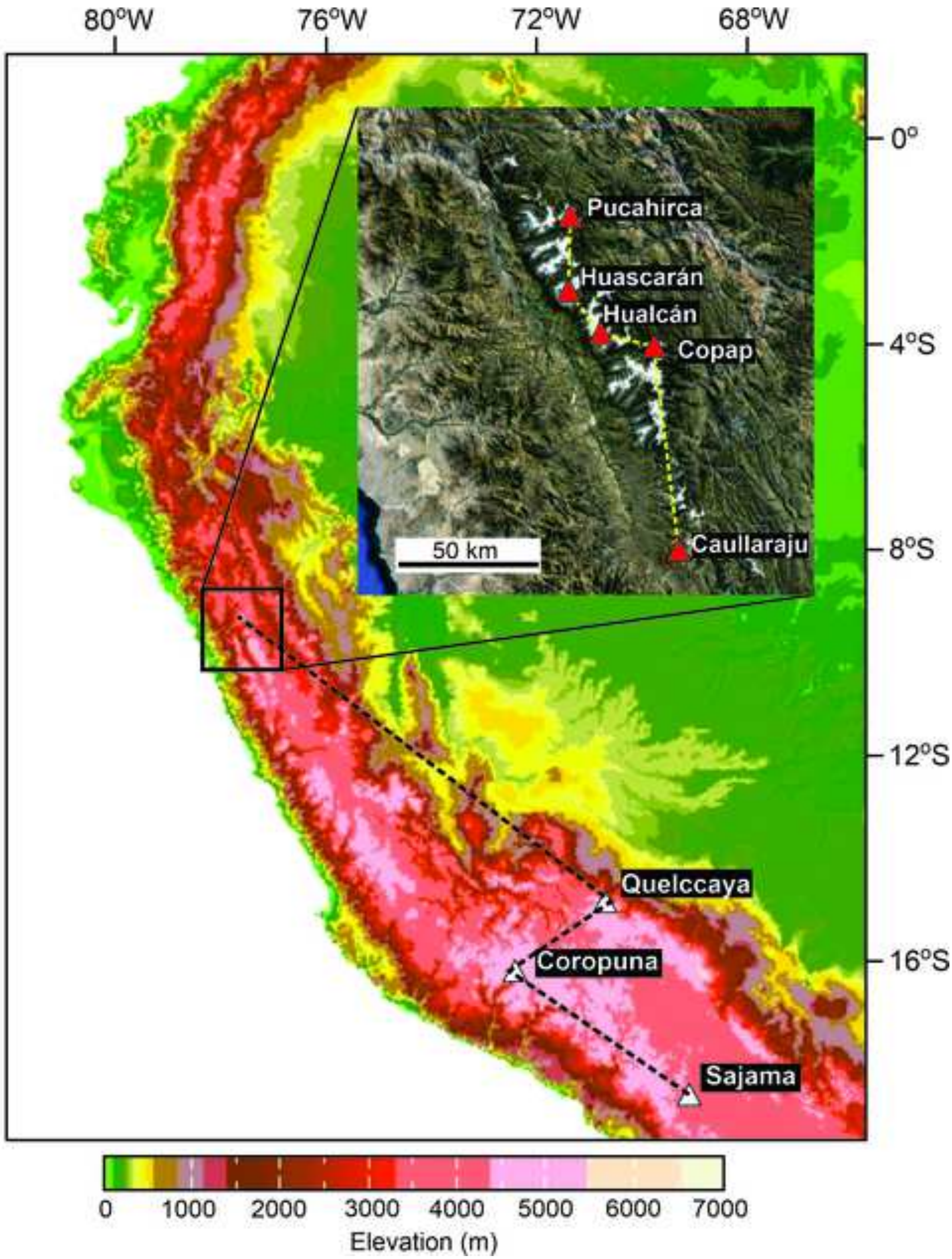

80°W
76°W
72°W
68°W
0°
4°S
8°S
12°S
16°S
Pucahirca
Huascarán
Hualcán
Copap
Caullaraju
50 km
Quelccaya
Coropuna
Sajama
0
1000
2000
3000
4000
5000
6000
7000
Elevation (m)

Figure 3

Figure 4

Click here to access/download;Figure;Figure 4.jpg

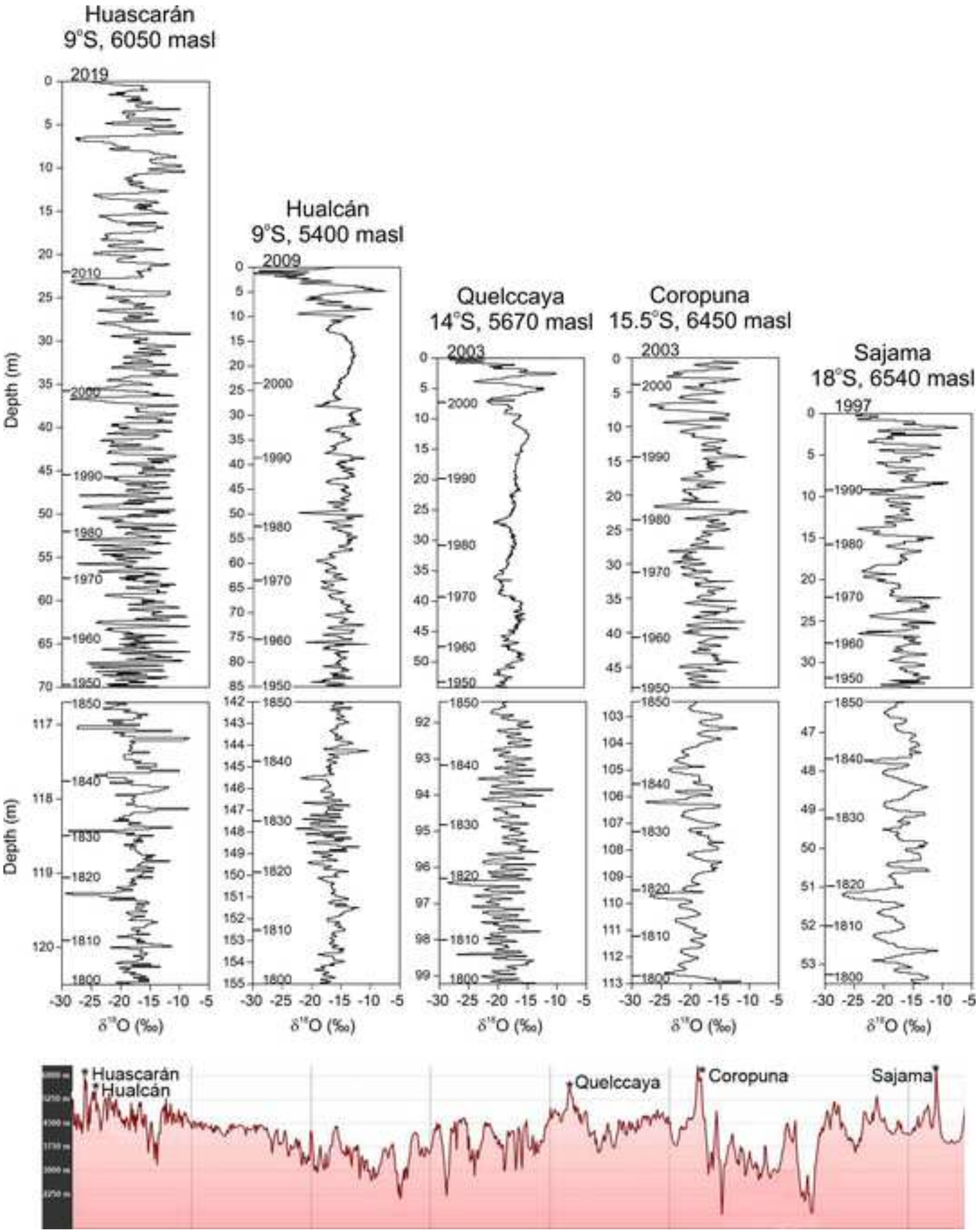

Figure 5

Click here to access/download;Figure;Figure 5.jpg

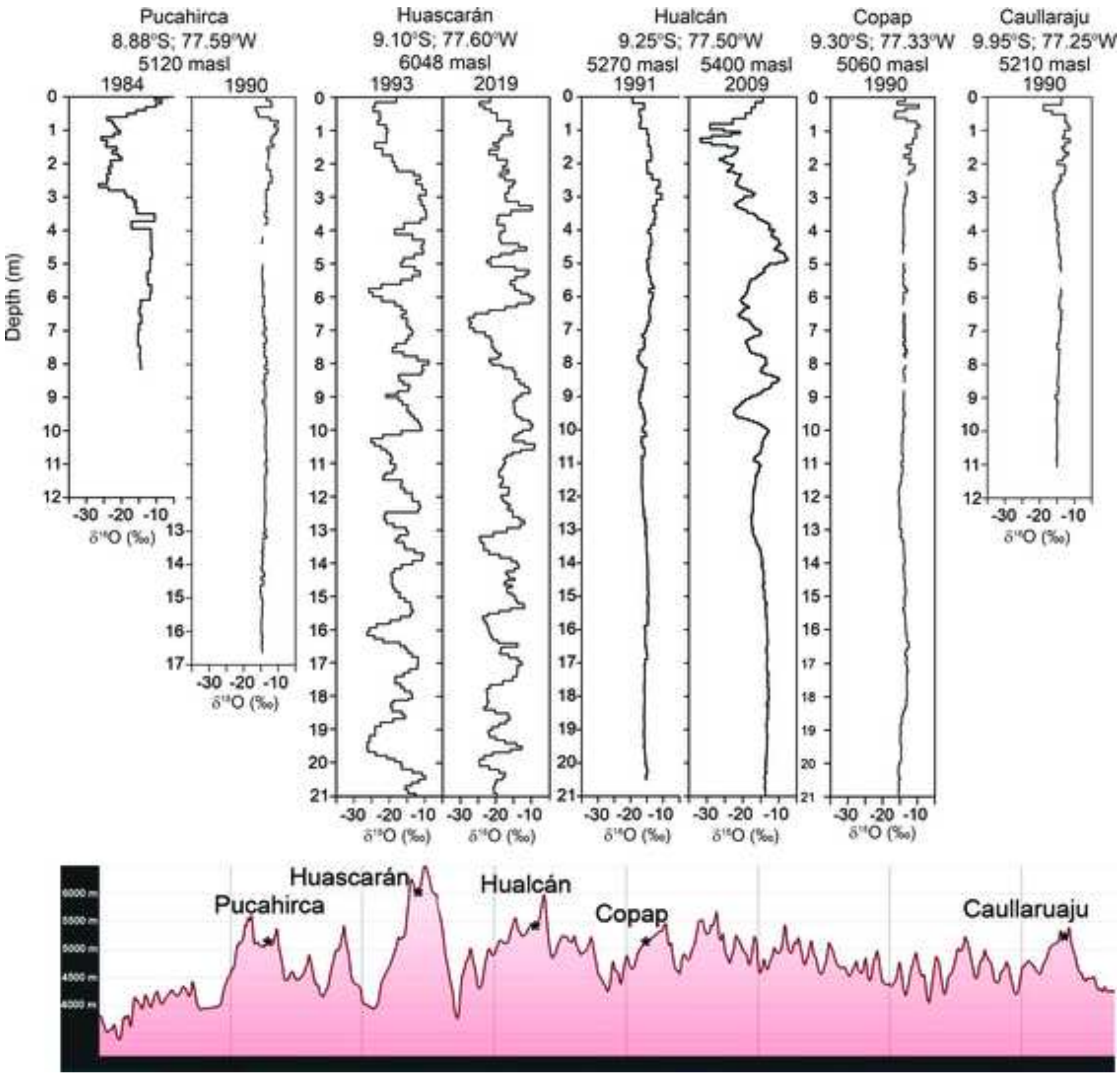

Figure 6

Click here to access/download;Figure;Figure 6.jpg

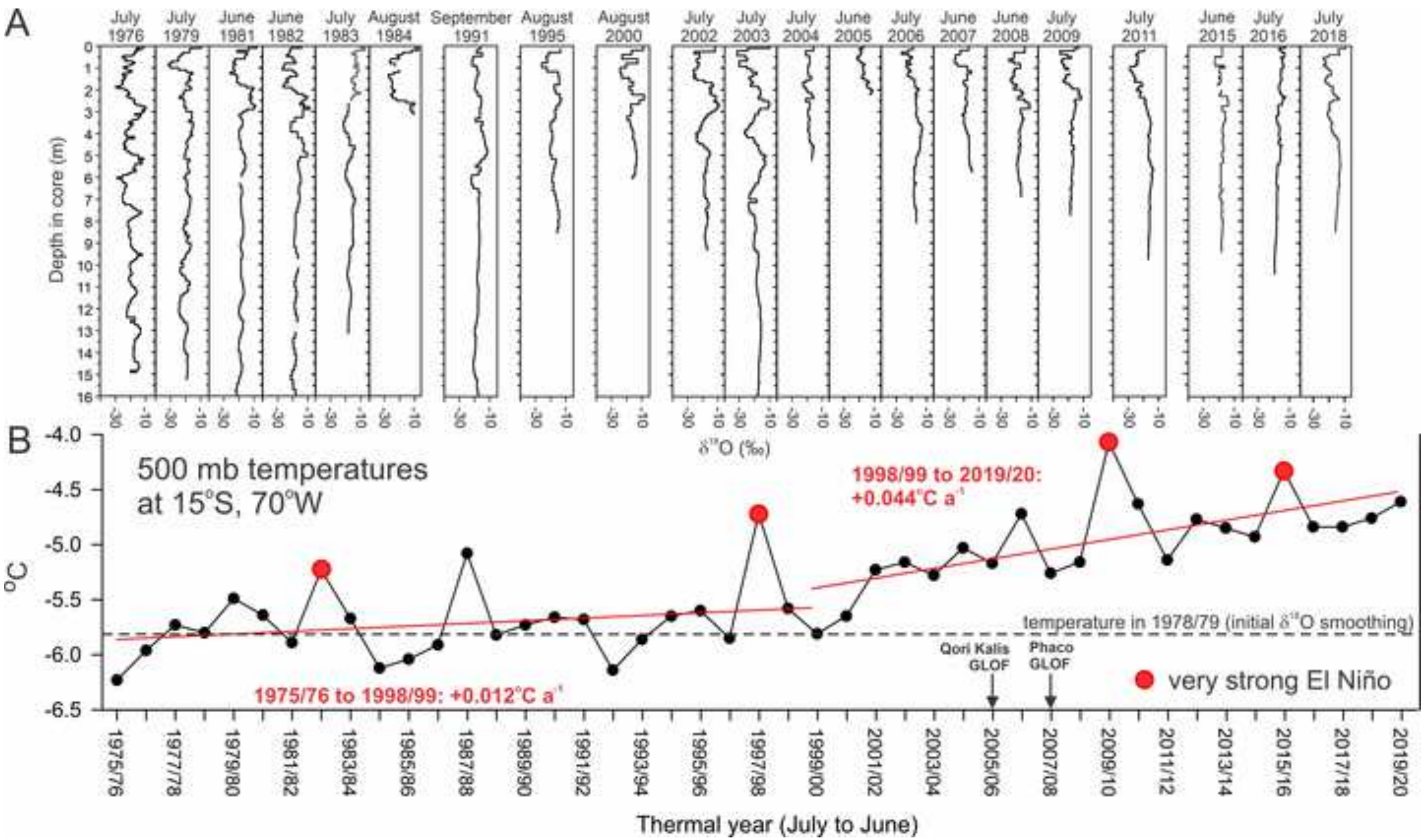

Figure 7

Click here to access/download;Figure;Figure 7.jpg

Figure 8

Click here to access/download;Figure;Figure 8.jpg

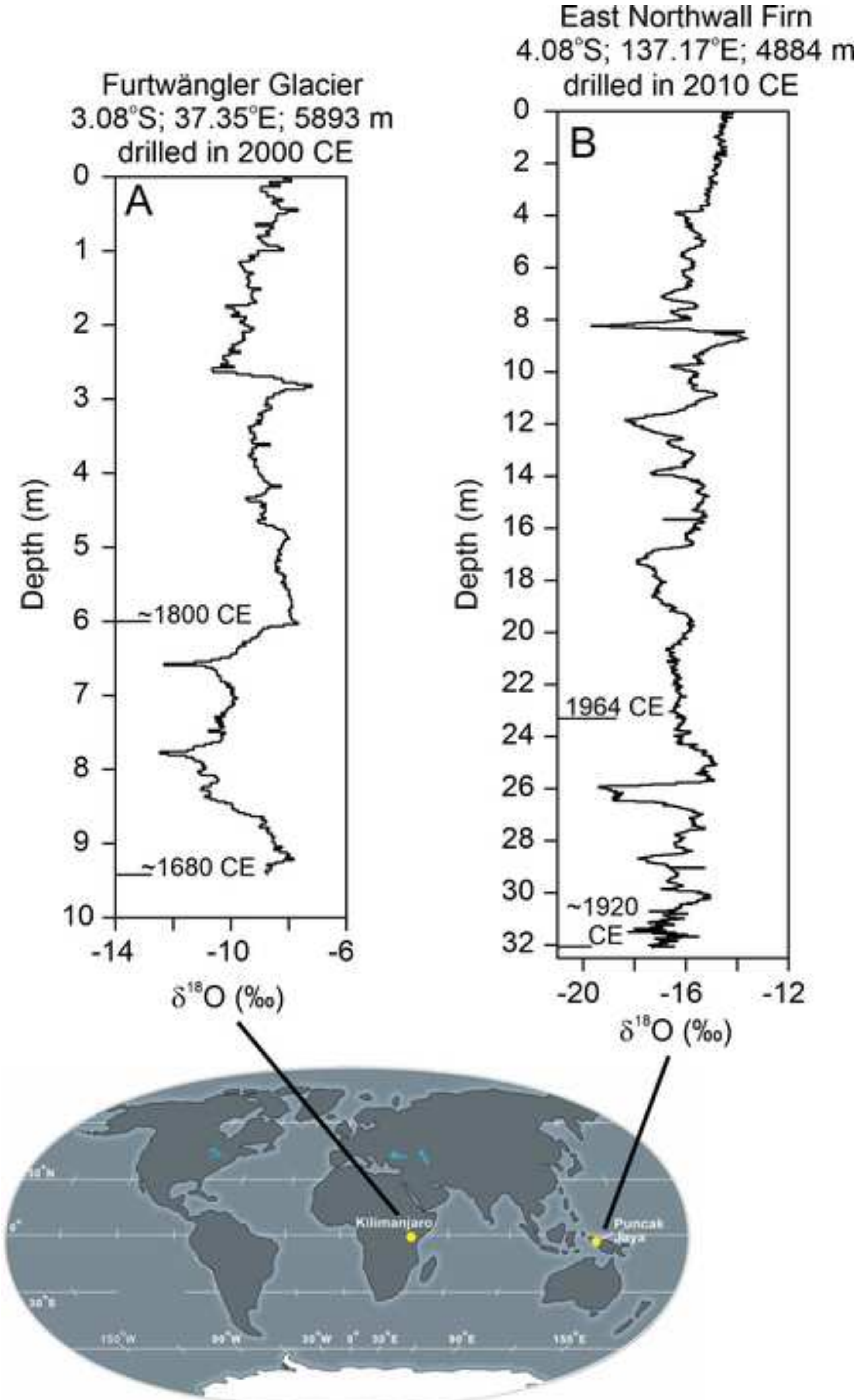

Figure 9

Click here to access/download;Figure;Figure 9.jpg

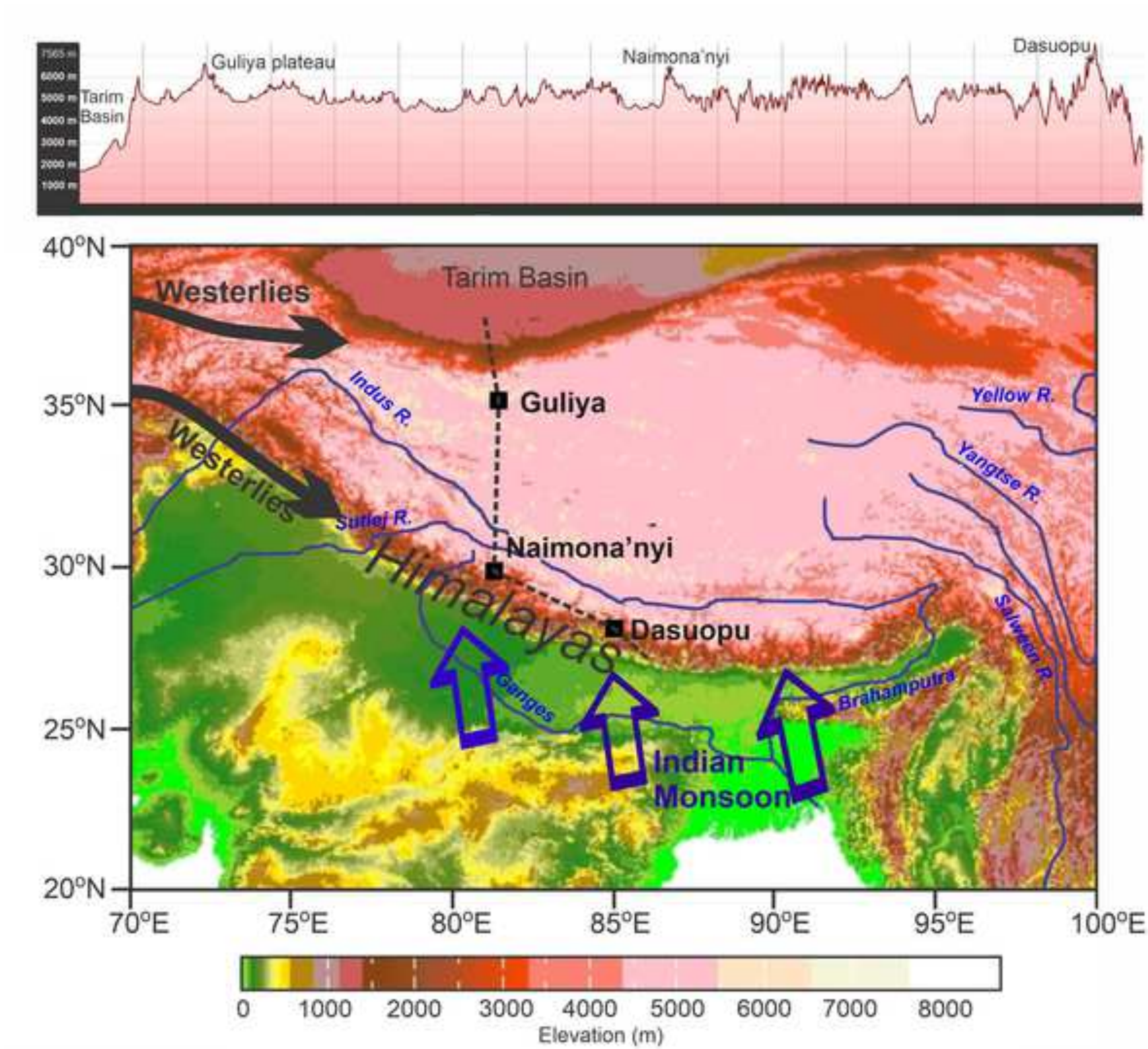

Figure 10

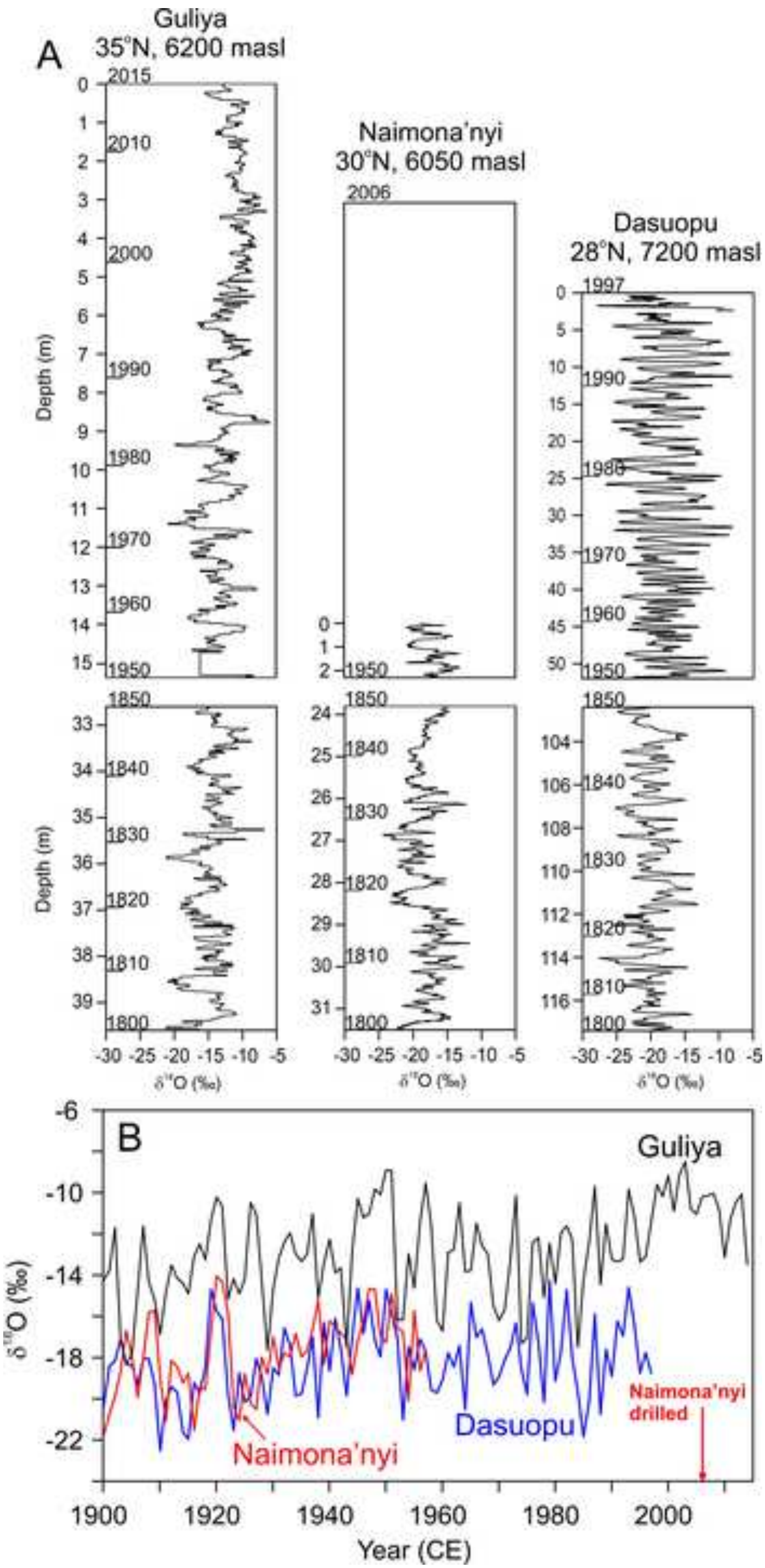
A
Guliya
35°N, 6200 masl
Naimona'nyi
30°N, 6050 masl
Dasuopu
28°N, 7200 masl
Depth (m)
δ¹⁸O (‰)
B
Guliya
Naimona'nyi
Dasuopu
Naimona'nyi drilled
δ¹⁸O (‰)
Year (CE)

Figure 11

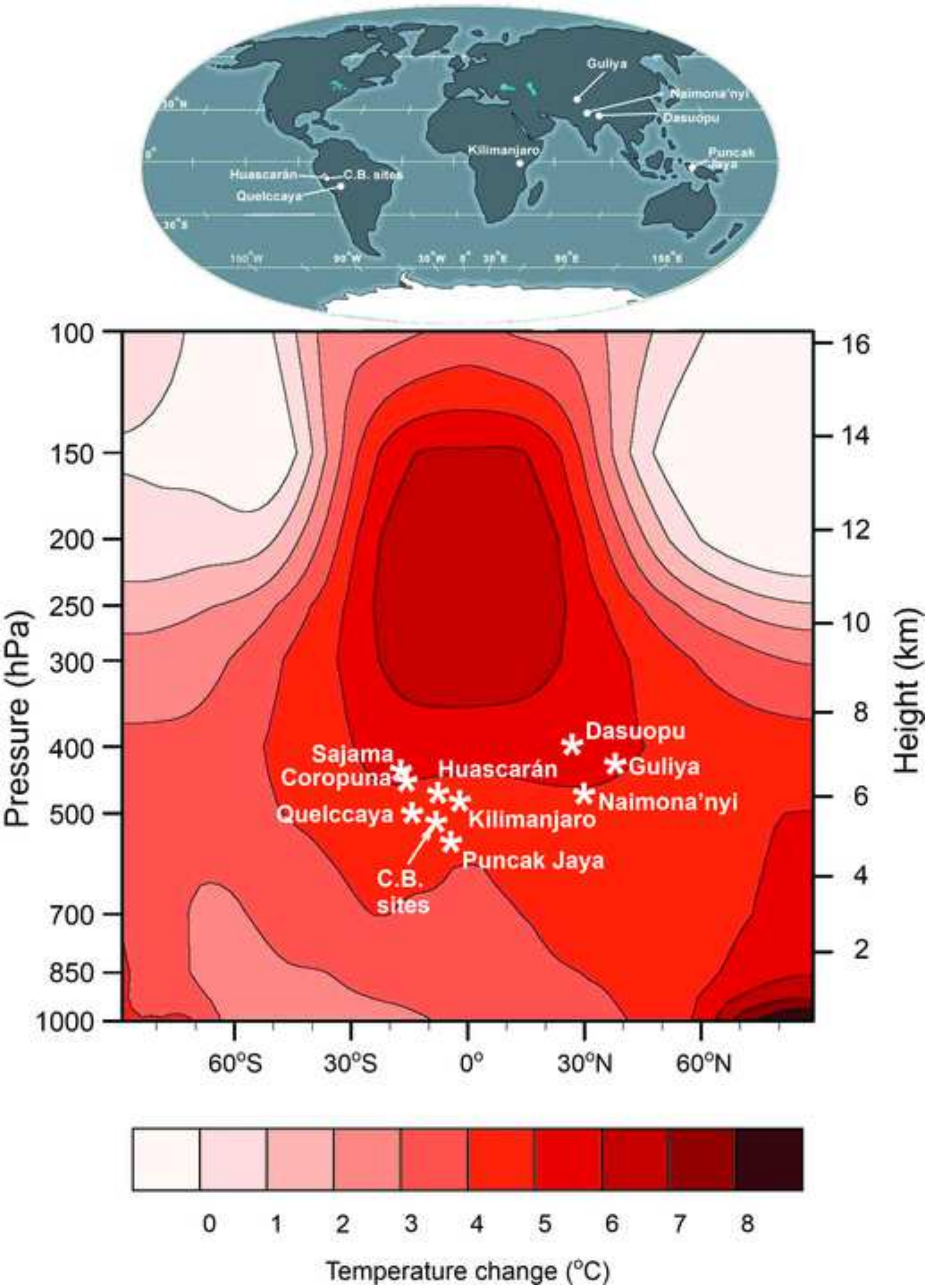
Guliya
Naimona'nyi
Dasuopu
Kilimanjaro
Puncak Jaya
Huascarán
C.B. sites
Quelccaya
Pressure (hPa)
Height (km)
Sajama
Coropuna
Huascarán
Dasuopu
Guliya
Naimona'nyi
Quelccaya
Kilimanjaro
Puncak Jaya
C.B. sites
100
150
200
250
300
400
500
700
850
1000
16
14
12
10
8
6
4
2
60°S
30°S
0°
30°N
60°N
0
1
2
3
4
5
6
7
8
Temperature change (°C)

Expression of competing interests

The authors declare that they have no known competing financial interests or personal relationships that could have appeared to influence the work reported in this paper.